

Synthesis of Group 4 Complexes That Contain the Tridentate Diamido/Donor Ligands [(ArylNCH₂CH₂)₂O]²⁻ and Zirconium Complexes That Contain [(ArylNCH₂CH₂)₂S]²⁻ and an Evaluation of Their Activity for the Polymerization of 1-Hexene

Michael Aizenberg, Laura Turculet, William M. Davis,
Florian Schattenmann, and Richard R. Schrock*

Department of Chemistry 6-331, Massachusetts Institute of Technology,
77 Massachusetts Avenue, Cambridge, Massachusetts 02139

Received June 22, 1998

Compounds of the type (ArylNHCH₂CH₂)₂O (Aryl = 2,6-Me₂C₆H₃ (H₂[**1a**]), 2,6-Et₂C₆H₃ (H₂[**1b**]), 2,6-*i*-Pr₂C₆H₃ (H₂[**1c**])) can be prepared by treating (TsOCH₂CH₂)₂O (TsO = tosylate) with the lithium anilides in THF. [**1a,b**]TiCl₂, [**1a,b**]TiMe₂, [**1a**]Ti(CH₂Ph)₂, [**1a-c**]M(NMe₂)₂ (M = Zr or Hf), [**1a-c**]MCl₂, and [**1a-c**]MR₂ (R = Me, Et, *i*-Bu) were prepared. An X-ray study of [**1a**]Ti(CH₂Ph)₂ revealed the structure to be a distorted trigonal bipyramid (type **B**) in which the two amido nitrogens and one benzyl ligand occupy equatorial positions. An X-ray study of [**1a**]ZrMe₂ showed it to be a distorted trigonal bipyramid that contains "axial" amido groups (type **A**), while an X-ray study of [**1c**]HfEt₂ revealed it to have a structure halfway between type **A** and type **B**, i.e., a distorted square pyramid with one alkyl in the apical position. Analogous compounds were also prepared that contain a sulfur donor instead of oxygen, i.e., [(2,6-Me₂C₆H₃NHCH₂CH₂)₂S] (H₂[**2a**]), [(2,6-*i*-Pr₂C₆H₃NHCH₂CH₂)₂S] (H₂[**2c**]), [**2a,c**]Zr(NMe₂)₂, [**2a,c**]ZrCl₂, [**2a,c**]ZrMe₂, and [**2c**]Zr(CH₂CHMe₂)₂. An X-ray study of [**2a**]ZrMe₂ revealed it to be closest to a type **B** structure. Addition of 1 equiv of [PhNMe₂H]-[B(C₆F₅)₄] in C₆D₅X (X = Br, Cl) to [**1a,c**]MMe₂ (M = Zr, Hf) gave cationic complexes that contain coordinated dimethylaniline, with which free aniline does not exchange readily on the NMR time scale at 60 °C. Addition of excess ether to {[**1a**]MMe(NMe₂Ph)}[B(C₆F₅)₄] (M = Zr, Hf) led to {[**1a**]MMe(ether)}[B(C₆F₅)₄] (M = Zr, Hf) complexes in high yield. Analogous cations can be prepared in the sulfur ligand system, but they do not appear to be as stable as in the oxygen ligand system. Zr and Hf dimethyl complexes that contain an oxygen donor or a sulfur donor ligand can be activated with [Ph₃C][B(C₆F₅)₄] to yield efficient catalysts for polymerization of 1-hexene, although the molecular weight of the poly(1-hexene) chains is limited to ~20 000–~25 000 under the conditions employed. Neither {[**1c**]ZrMe(ether)}[B(C₆F₅)₄] nor {[**1c**]HfMe(ether)}[B(C₆F₅)₄] will polymerize 1-hexene in C₆D₅Br at room temperature, and neither will polymerize ethylene readily at 1 atm and 25 °C. It is proposed that a solvated five-coordinate cation must lose the solvent in order to react with an olefin and that β-hydride elimination in the four-coordinate cation limits chain length.

Introduction

Significant advances have been made in the synthesis of "well-defined" olefin polymerization catalysts of the early metals (largely group 4) in the last 15 years, the vast majority of which contain two cyclopentadienyl-like rings or, more recently, one cyclopentadienyl-like ring.^{1–4} The active species in such complexes is now widely regarded to be a group 4 metal cation formed in the presence of a "weakly coordinating" anion such as [B(C₆F₅)₄]⁻. However, in the past decade in particular researchers have been looking for group 4 metal cations that do not have one or more cyclopentadienyl rings

bound to the metal.⁵ Most recently group 4 complexes that contain chelating diamido ligand systems have received increased attention as potential olefin polymerization catalysts.^{6–32} Two systems of greatest interest, largely because of their ability to behave as living

- (1) Brintzinger, H. H.; Fischer, D.; Mulhaupt, R.; Rieger, B.; Waymouth, R. M. *Angew. Chem., Int. Ed. Engl.* **1995**, *34*, 1143.
- (2) Kaminsky, W.; Arndt, M. *Adv. Polym. Sci.* **1997**, *127*, 144.
- (3) Bochmann, M. *J. Chem. Soc., Dalton Trans.* **1996**, 255.
- (4) Chen, Y.-X.; Marks, T. J. *Organometallics* **1997**, *16*, 3649.

- (5) For leading references see: (a) Martin, A.; Uhrhammer, R.; Gardner, T. G.; Jordan, R. F.; Rogers, R. D. *Organometallics* **1998**, *17*, 382. (b) Bei, X. H.; Swenson, D. C.; Jordan, R. F. *Organometallics* **1997**, *16*, 3282. (c) Tjaden, E. B.; Swenson, D. C.; Jordan, R. F.; Petersen, J. L. *Organometallics* **1995**, *14*, 371.

- (6) Scollard, J. D.; McConville, D. H. *J. Am. Chem. Soc.* **1996**, *118*, 10008.

- (7) Scollard, J. D.; McConville, D. H.; Payne, N. C.; Vittal, J. J. *Macromolecules* **1996**, *29*, 5241.

- (8) Scollard, J. D.; McConville, D. H.; Vittal, J. J. *Organometallics* **1995**, *14*, 5478.

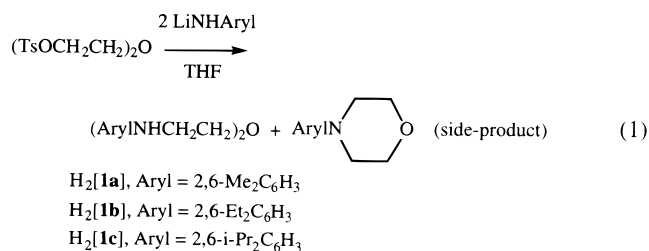
- (9) Scollard, J. D.; McConville, D. H.; Rettig, S. J. *Organometallics* **1997**, *16*, 1810.

- (10) Aoyagi, K.; Gantzel, P. K.; Kalai, K.; Tilley, T. D. *Organometallics* **1996**, *15*, 923.

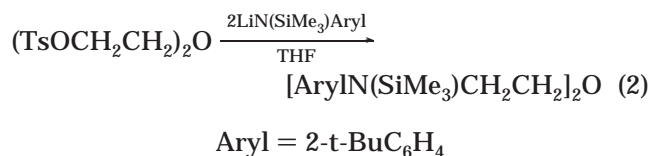
polymerization catalysts, are dialkyl complexes of titanium that contain diamido ligands such as $[\text{ArylNCH}_2\text{CH}_2\text{CH}_2\text{NAr}]^{2-}$ (Aryl = 2,6-*i*-Pr₂C₆H₃),^{6–9} and dialkyl complexes of zirconium that contain the “diamido/donor” ligand $[\text{((}t\text{-Bu-}d_6\text{)N-}o\text{-C}_6\text{H}_4\text{)}_2\text{O}]^{2-}$ ([NON]²⁻).^{11,12} The living intermediates in the latter system are stable in the absence of 1-hexene and have been observed in ¹³C labeling experiments to be consistent with 1,2-insertion of the olefin into the metal–carbon bond.¹² We recently reported in a preliminary fashion complexes that contain “diamido/donor” variations of the [NON]²⁻ ligand, $[(2,6\text{-R}_2\text{C}_6\text{H}_3\text{NCH}_2\text{CH}_2)_2\text{O}]^{2-}$ (R = Me, *i*-Pr), and preliminary experiments concerning their use as catalysts for the polymerization of 1-hexene.²⁵ In this paper we report the full details of studies concerning complexes of Ti, Zr, and Hf that contain a tridentate ligand of the general formula $[(\text{ArylNCH}_2\text{CH}_2)_2\text{O}]^{2-}$, along with more abbreviated related studies of zirconium complexes that contain a tridentate ligand of the general formula $[(\text{ArylNCH}_2\text{CH}_2)_2\text{S}]^{2-}$.

Results

Synthesis of Complexes That Contain $[(\text{ArylNCH}_2\text{CH}_2)_2\text{O}]^{2-}$ Ligands. Compounds of the type $(\text{ArylNHCH}_2\text{CH}_2)_2\text{O}$ (Aryl = 2,6-Me₂C₆H₃, 2,6-Et₂C₆H₃, 2,6-*i*-Pr₂C₆H₃) can be prepared by treating $(\text{TsOCH}_2\text{CH}_2)_2\text{O}$ (TsO = tosylate) with the lithium anilides in THF (eq 1). The crude products, which are sufficiently pure for further use, are produced in 50–80% yield as oils ($\text{H}_2[1\mathbf{b}]$ or $\text{H}_2[1\mathbf{c}]$) or as a crystalline solid ($\text{H}_2[1\mathbf{a}]$). The side products, N-substituted morpholines, can be

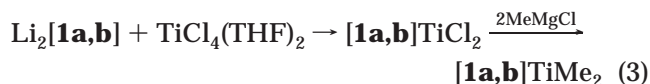


separated readily from the $(\text{ArylNHCH}_2\text{CH}_2)_2\text{O}$ products. The N-substituted morpholine is the major product when Aryl = 2-*t*-BuC₆H₄ because of the facile intramolecular displacement of the second tosyl group after the first substitution. Therefore, the anilide must be protected first with a trimethylsilyl group, which then allows the protected product to be synthesized in good yield (eq 2). Subsequent hydrolysis with aqueous

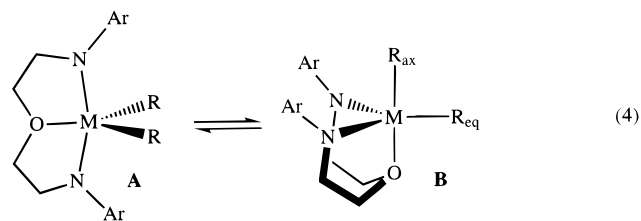


HCl yields (2-*t*-BuC₆H₄NHCH₂CH₂)₂O ($\text{H}_2[1\mathbf{d}]$) in an overall yield of 50%.

The reaction between $\text{TiCl}_4(\text{THF})_2$ and 2 equiv of $\text{Li}_2[1\mathbf{a}]$ or $\text{Li}_2[1\mathbf{b}]$ (prepared in situ) gave the titanium dichloride complexes $[1\mathbf{a}]\text{TiCl}_2$ and $[1\mathbf{b}]\text{TiCl}_2$, respectively (eq 3). The dichloride complexes react smoothly



with methyl Grignard reagent to yield the titanium dimethyl complexes $[1\mathbf{a,b}]\text{TiMe}_2$ as yellow to yellow-brown powders. Proton and carbon NMR spectra of $[1\mathbf{a}]\text{TiMe}_2$ and $[1\mathbf{b}]\text{TiMe}_2$ are consistent with species that contain two mirror planes on the NMR time scale. Sharp singlet resonances belonging to the methyl groups bound to titanium are found in the proton NMR spectrum at 0.90 and 0.89 ppm and in the carbon NMR spectrum at 60.75 and 61.14 ppm, for $[1\mathbf{a}]\text{TiMe}_2$ and $[1\mathbf{b}]\text{TiMe}_2$, respectively. In $[1\mathbf{a}]\text{TiMe}_2$ the two methyl groups are still equivalent on the NMR time scale at -70°C (toluene-*d*₈, 500 MHz). On the basis of these data we cannot determine if the ground-state structure is of type **A** or type **B** for $[1\mathbf{a}]\text{TiMe}_2$ and $[1\mathbf{b}]\text{TiMe}_2$ (eq 4). If the lowest energy structure is of type **B**, which



would be analogous to the structure of $[1\mathbf{a}]\text{Ti}(\text{CH}_2\text{Ph})_2$ (see below), then a structure of type **A** must be readily accessible by a Berry-type process in which the two equatorial amido nitrogens swing into axial positions while R_{ax} and the oxygen donor end up in equatorial positions. As we shall see, structures **A** and **B** are close

(11) Baumann, R.; Davis, W. M.; Schrock, R. R. *J. Am. Chem. Soc.* **1997**, *119*, 3830.

(12) Baumann, R.; Schrock, R. R. *J. Organomet. Chem.* **1998**, *557*, 69.

(13) Horton, A. D.; de With, J.; van der Linden, A. J.; van de Weg, H. *Organometallics* **1996**, *15*, 2672.

(14) Horton, A. D.; de With, J. *Chem. Commun.* **1996**, 1375.

(15) Cloke, F. G. N.; Geldbach, T. J.; Hitchcock, P. B.; Love, J. B. *J. Organomet. Chem.* **1996**, *506*, 343.

(16) Cloke, F. G. N.; Hitchcock, P. B.; Love, J. B. *J. Chem. Soc., Dalton Trans.* **1995**, 25.

(17) Clark, H. C. S.; Cloke, F. G. N.; Hitchcock, P. B.; Love, J. B.; Wainwright, A. P. *J. Organomet. Chem.* **1995**, *501*, 333.

(18) Warren, T. H.; Schrock, R. R.; Davis, W. M. *Organometallics* **1996**, *15*, 562.

(19) Warren, T. H.; Schrock, R. R.; Davis, W. M. *Organometallics* **1998**, *17*, 308.

(20) Guérin, F.; McConville, D. H.; Vittal, J. J. *Organometallics* **1997**, *16*, 1491.

(21) Guérin, F.; McConville, D. H.; Payne, N. C. *Organometallics* **1996**, *15*, 5085.

(22) Guérin, F.; McConville, D. H.; Vittal, J. J. *Organometallics* **1995**, *14*, 3154.

(23) Guérin, F.; McConville, D. H.; Vittal, J. J. *Organometallics* **1996**, *15*, 5586.

(24) Gibson, B. C.; Kimberley, B. S.; White, A. J. P.; Williams, D. J.; Howard, P. *Chem. Commun.* **1998**, 313.

(25) Schrock, R. R.; Schattenmann, F.; Aizenberg, M.; Davis, W. M. *Chem. Commun.* **1998**, 199.

(26) Male, N. A. H.; Thornton-Pett, M.; Bochmann, M. *J. Chem. Soc., Dalton Trans.* **1997**, 2487.

(27) Herrmann, W. A.; Denk, M.; Albach, R. W.; Behm, J.; Herdtweck, E. *Chem. Ber.* **1991**, *124*, 683.

(28) Kempe, R.; Brenner, S.; Arndt, P. *Organometallics* **1996**, *15*, 1071.

(29) Friedrich, S.; Schubart, M.; Gade, L. H.; Scowen, I. J.; Edwards, A. J.; McPartlin, M. *Chem. Ber.-Recl.* **1997**, *130*, 1751.

(30) Tsuie, B.; Swenson, D. C.; Jordan, R. F.; Petersen, J. L. *Organometallics* **1997**, *16*, 1392.

(31) Tinkler, S.; Deeth, R. J.; Duncalf, D. J.; McCamley, A. *Chem. Commun.* **1996**, 2623.

(32) Schattenmann, F.; Schrock, R. R.; Davis, W. M. *Organometallics* **1998**, *17*, 989.

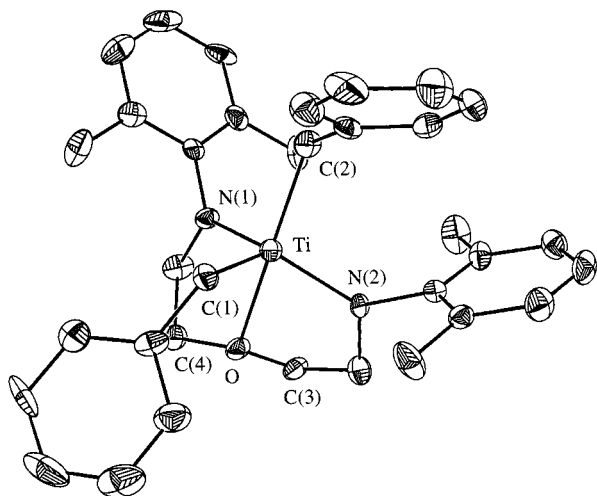


Figure 1. ORTEP drawing of the structure of **[1a]Ti(CH₂C₆H₅)₂**.

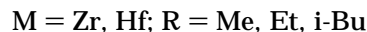
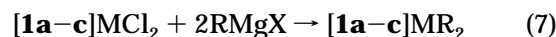
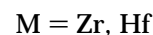
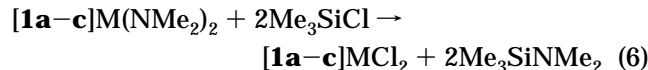
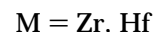
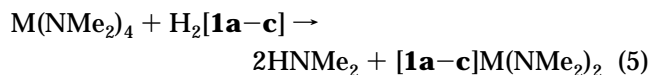
in energy; therefore, the titanium dimethyl and dibenzyl complexes may not have similar structures.

Red, crystalline **[1a]Ti(CH₂Ph)₂** can be prepared in a slow reaction between Ti(CH₂Ph)₄ and H₂**[1a]**, although the isolated yield is low (~15%). It was also prepared in ~35% isolated yield (on a small scale and not optimized) by treating **[1a]TiCl₂** with 2 equiv of benzyl Grignard reagent. Its 300 MHz room-temperature proton NMR spectrum exhibits broad resonances for the benzyl groups ($\delta(H_{\text{ar}}) \sim 2.32$ ppm) and somewhat broadened resonances for the protons of the backbone and the ligand methyl groups. In the room-temperature ¹³C-¹H spectrum, measured at either 75 or 125 MHz, all resonances can be observed except that for the benzylic carbon of the titanium-bound benzyl groups. At 65 °C a benzylic carbon resonance can be observed as a broad singlet at δ 91.7 ppm (125 MHz, C₆D₆). At -70 °C (500 MHz in toluene-*d*₈) the proton NMR spectrum is consistent with a static structure on the NMR time scale in which two different benzyl groups are present, although its complexity prevented ready assignment of all resonances.

An X-ray study of **[1a]Ti(CH₂Ph)₂** (Figure 1, Tables 1 and 2) confirmed the structure to be one of type **B**; the two nitrogens and one benzyl ligand (C(1)) occupy "equatorial" positions, while the oxygen and another benzyl group (C(2)) occupy approximately axial sites. In accord with this description, the C(2)-Ti-O angle is 169.3(3)° while the C(1)-Ti-O angle is only 92.4(3)°. The latter should be compared with the O-Ti-N(1) angle (76.1(3)°) and the O-Ti-N(2) angle (75.2(3)°). The sum of angles around the Ti center in the equatorial plane equals 351.6(3)°. The Ti-C(1) and Ti-C(2) bond lengths (2.129(10) and 2.118(8) Å) are statistically indistinguishable and close to the values observed in [(*t*-BuN-*o*-C₆H₄)₂O]TiMe₂,¹¹ while both equatorial Ti-N bond lengths (1.940(7) and 1.962(6) Å) are in the range of other Ti-amido bond lengths reported recently (1.84-1.98 Å).^{10,11,21,29,31} The Ti-N-C bond angles (127.0(5) and 129.4(6)°) are larger than corresponding angles in other structures to be discussed below, which is perhaps evidence of a greater degree of steric crowding in the "coordination pocket" of **[1a]Ti(CH₂Ph)₂**. The Ti-O bond length is substantially shorter in **[1a]Ti(CH₂Ph)₂** (2.224(5) Å) than in [(*t*-BuN-*o*-C₆H₄)₂O]TiMe₂ (2.402(4)

Å), perhaps in part as a consequence of the greater donor ability of the dialkyl ether oxygen, although differences associated with different degrees of flexibility of the diamido/donor ligand backbone in [(*t*-BuN-*o*-C₆H₄)₂O]TiMe₂ and **[1a]Ti(CH₂Ph)₂** cannot be discounted. Somewhat surprisingly, both benzyl ligands are bound in an η^1 fashion, as evidenced by the values of the angles Ti-C(1)-C (122.9(6)°) and Ti-C(2)-C (121.0(6)°). These structural features suggest that the relatively complex set of resonances observed in solution at low temperature in the ¹H NMR spectrum of **[1a]Ti(CH₂Ph)₂** does *not* involve formation of an η^x -CH₂-Ph ligand where $x > 1$ and, furthermore, that the relatively slow equilibration of the benzyl groups in **[1a]-Ti(CH₂Ph)₂** relative to the methyl groups in **[1a]TiMe₂** might be ascribed to a greater degree of steric crowding in an intermediate structure of type **A** for **[1a]Ti(CH₂-Ph)₂** than in a structure of type **A** for **[1a]TiMe₂**. The angle between the N(1)-Ti-O and N(2)-Ti-O planes is 137°, 17° larger than in an ideal trigonal bipyramid, as a consequence of repulsion between the two substituted amido nitrogen atoms. This angle can be employed as a measure of the structural type (A or B).

The reaction between M(NMe₂)₄ (M = Zr, Hf) and H₂-**[1a-c]** produced the white crystalline **[1a-c]M(NMe₂)₂** complexes in high yield (eq 5). The **[1a-c]M(NMe₂)₂**



complexes react with an excess of Me₃SiCl in ether to form relatively insoluble **[1a-c]MCl₂** complexes (eq 6). The relatively low solubility of the **[1a-c]MCl₂** species suggests that they may be dimers in the solid state, as is true of {[NON]ZrCl₂}₂.³³ Finally, the **[1a-c]MCl₂** species can be alkylated by Grignard reagents to afford the corresponding dialkyl complexes **[1a-c]MR₂** (R = Me, Et, i-Bu) in excellent yield (eq 7). The isobutyl species are stable at room temperature both in the solid state and in solution, which suggests that they are not prone to facile decomposition by β -hydride processes, e.g., to give isobutane and "[**1a**]M(CH₂CMe₂)," or by γ -hydride abstraction or elimination processes. Several exceptions to these general reactivity patterns should be mentioned. Attempts to prepare complexes that contain the unsymmetrical ligand H₂**[1d]** invariably led to mixtures of isomers for bis(dimethylamido), dichloride, and dimethyl complexes; NMR spectra suggest that they are mixtures of meso and racemic species formed as a consequence of restricted rotation (on the NMR time scale) around the N-C_{ipso} bond. Full assignment of NMR spectra therefore was impractical. We do not

(33) Baumann, R.; Schrock, R. R.; Davis, W. M. Unpublished results.

Table 1. Crystallographic Data, Collection Parameters, and Refinement Parameters for [1a]Ti(CH₂Ph)₂, [1a]ZrMe₂, [1c]HfEt₂, and [2a]ZrMe₂^a

	[1a]Ti(CH ₂ Ph) ₂	[1a]ZrMe ₂	[1c]HfEt ₂	[2a]ZrMe ₂
empirical formula	C ₃₄ H ₄₀ N ₂ O ₂ Ti	C ₂₂ H ₃₂ N ₂ OZr	C ₃₂ H ₅₂ N ₂ O ₂ Hf	C ₂₂ H ₃₂ N ₂ SZr
fw	540.58	431.73	659.27	447.79
cryst color	red	colorless	colorless	colorless
cryst dimens (mm)	0.18 × 0.10 × 0.08	0.20 × 0.20 × 0.12	0.40 × 0.25 × 0.25	0.20 × 0.20 × 0.20
cryst syst	orthorhombic	orthorhombic	monoclinic	monoclinic
a (Å)	32.803(8)	12.741(3)	12.396(2)	11.143(3)
b (Å)	42.342(13)	22.663(5)	16.662(4)	14.812(3)
c (Å)	8.547(4)	7.518(2)	16.306(4)	13.976(3)
α (deg)	90	90	90	90
β (deg)	90	90	109.70(2)	105.84(2)
γ (deg)	90	90	90	90
V (Å ³), Z	11872(7), 16	2170.9(8), 4	3170.8(11), 4	2219.2(8), 4
space group	<i>Fdd2</i>	<i>Pnma</i>	<i>P2₁/c</i>	<i>P2₁/c</i>
D _{calcd} (Mg/m ³)	1.210	1.321	1.381	1.340
μ (mm ⁻¹)	0.316	0.519	3.314	0.597
F ₀₀₀	4608	904	1352	936
no. of rflns collected	6849	8145	12802	8920
no. of indep rflns	2636	1607	4534	3189
R _{int}	0.0888	0.0703	0.0282	0.0419
data/restraints/param	25071/344	1606/0/125	4530/0/326	3187/0/236
R1 [<i>I</i> > 2σ(<i>I</i>)]	0.0609	0.0368	0.0202	0.0321
wR2	0.1269	0.1009	0.0526	0.0864
GOF on F ²	1.095	1.179	1.086	1.137

^a All data were collected on a Siemens SMART/CCD diffractometer with λ(Mo Kα) = 0.710 73 Å using ω scans at 183(2) K and solved using a full-matrix least-squares refinement on F². No absorption correction was applied in any case.

Table 2. Selected Bond Lengths (Å) and Angles (deg) in [1a]Ti(CH₂Ph)₂, [1a]ZrMe₂, [1c]HfEt₂, and [2a]ZrMe₂^a

	[1a]Ti(CH ₂ Ph) ₂	[1a]ZrMe ₂	[1c]HfEt ₂	[2a]ZrMe ₂
M–N1	1.962(6)	2.084(3)	2.087(3)	2.073(3)
M–N2	1.940(7)	2.084(3)	2.081(3)	2.067(3)
M–C1	2.129(10)	2.255(6)	2.232(4)	2.261(3)
M–C2	2.118(8)	2.253(6)	2.224(4)	2.279(3)
M–D	2.224(5)	2.336(3)	2.343(2)	2.8046(9)
N1–M–N2	128.6(3)	139.1(2)	136.37(11)	125.27(10)
N1–M–C1	109.2(3)	102.9(1)	104.09(12)	112.58(12)
N1–M–C2	96.6(3)	103.1(1)	101.68(13)	102.06(11)
N1–M–D	76.1(3)	69.54(9)	70.66(10)	71.49(7)
N2–M–C1	113.8(3)	102.9(1)	103.33(13)	110.46(12)
N2–M–C2	104.3(3)	103.1(1)	103.75(14)	100.91(11)
N2–M–D	75.2(3)	69.54(9)	70.52(10)	70.55(7)
C1–M–C2	97.4(4)	100.0(2)	104.0(2)	101.37(13)
C1–M–D	92.4(3)	129.7(2)	103.05(11)	97.96(10)
C2–M–D	169.3(3)	130.2(2)	152.89(13)	160.60(9)
C3–D–C4	113.3(7)	113.7(4)	113.2(3)	105.0(2)
M–D–C4	111.4(5)	114.9(2)	116.2(2)	88.42(11)
M–D–C3	107.9(5)	114.9(2)	115.7(2)	99.44(11)
M–N1–C	127.0(5)	120.2(2)	120.1(2)	110.1(2)
M–N2–C	129.4(6)	120.2(2)	120.1(2)	116.4(2)
M–C1–C	122.9(6)		112.7(2)	
M–C2–C	121.0(6)		117.1(3)	
N1–M–D/ N2–M–D ^b	137	180	160	140

^a D = donor (O or S); M = Ti, Zr, Hf. ^b The external angles between the planes, ideally 120° in type B, 180° in type A; obtained from a Chem 3D model.

know whether *meso* and *rac* isomers are configurationally stable on the *chemical* time scale at room temperature. The reaction between [1a]ZrCl₂ and 2 equiv of Me₃CCH₂MgCl gave only [1a]Zr(CH₂CMe₃)Cl, while [1a]Zr(CH₂CMe₃)₂ was formed using neopentyl lithium as an alkylating reagent. This behavior is a fairly typical consequence of some resistance to formation of a relatively crowded dialkyl species using the Grignard reagent, a generally “weaker” alkylating agent than a lithium reagent.

The ¹H and ³¹C{¹H} NMR spectra of the Zr and Hf diamido, dichloro, and dialkyl complexes are entirely analogous. The most noteworthy NMR spectral features are the following: (i) the protons of the OCH₂CH₂N

backbone are found as two separate triplet resonances (sometimes distorted toward an AB pattern) for the dimethylamido and dichloride complexes, while for the dialkyl complexes these resonances are observed as two second-order multiplets; (ii) only one set of resonances for two metal-bound dimethylamido or alkyl groups is observed in both proton and carbon NMR spectra, indicative of either a structure in which two mirror planes are present (type **A**) or a process that rapidly interconverts two type **B** structures via a type **A** intermediate on the NMR time scale; (iii) all complexes that contain the [1c]²⁻ ligand reveal two sets of resonances for the isopropyl methyl protons but only one resonance belonging to the methine protons, consistent

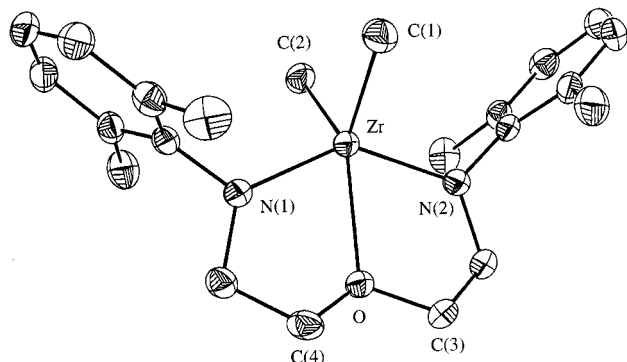


Figure 2. ORTEP drawing of the structure of $[1a]Zr(CH_3)_2$.

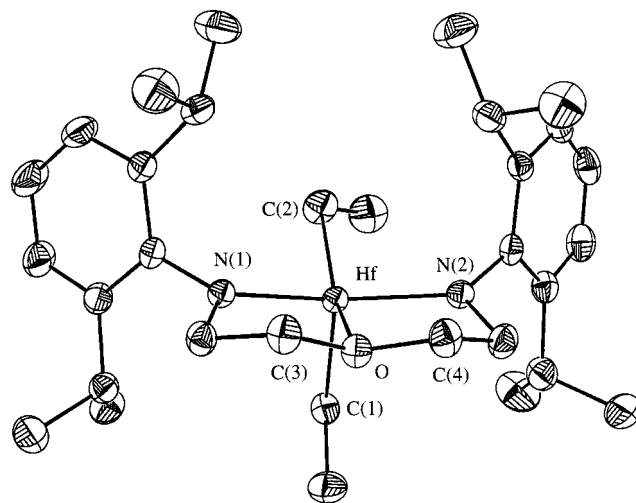


Figure 3. ORTEP drawing of the structure of $[1c]Hf(CH_2CH_3)_2$.

with the presence of a mirror plane that interconverts aryl rings and with hindered rotation of aryl rings about N–C_{ipso} bonds on the NMR time scale.

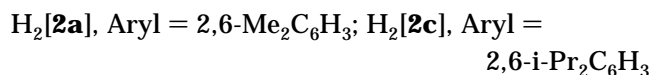
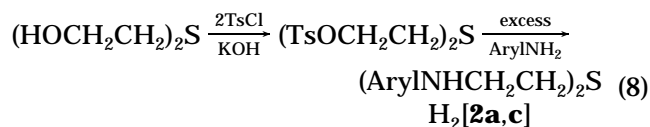
An X-ray study of $[1a]ZrMe_2$ (Figure 2, Tables 1 and 2) shows it to be a type **A** structure in which a mirror plane is defined by Zr, O, C(1), and C(2). None of the Zr–ligand bond lengths is unusual, being $\sim 0.12(1)$ Å longer than in $[1a]Ti(CH_2Ph)_2$, as one would expect. The two zirconium-bound methyl groups are technically inequivalent, as a consequence of the fact that the oxygen donor is not planar (the sum of the angles around O is 343.5°), but the Zr–C(1) and Zr–C(2) bond lengths are statistically identical, as are the O–Zr–C(1) and O–Zr–C(2) angles, and there is no evidence that any structure of lower than C_{2v} symmetry on the NMR time scale is accessible down to $-80^\circ C$. The angle between the N(1)–M–O and N(2)–M–O planes in $[1a]ZrMe_2$ is 180° , which is characteristic of a structure of type **A**. Interestingly, the C(1)–M–C(2) angles in $[1a]ZrMe_2$ and $[1a]Ti(CH_2Ph)_2$ are within 3° of one another. Therefore, the process of converting a structure of type **B** to a structure of type **A** could be viewed as a “rotation” of the C(1)–M–C(2) unit in the C(1)–M–O–C(2) plane as the angle between the N(1)–M–O and N(2)–M–O planes increases from 137 to 180° .

An X-ray study of $[1c]HfEt_2$ (Figure 3, Tables 1 and 2) suggests that this molecule is best described as a distorted square pyramid with C(1) in the apical position and C(2), N(1), N(2), and O in the basal plane. The core

of this structure is approximately halfway between the core structure of $[1a]ZrMe_2$ and that of $[1a]Ti(CH_2Ph)_2$, as shown by the angle between the N(1)–M–O and N(2)–M–O planes (160°), which is virtually halfway between the corresponding angles in $[1a]ZrMe_2$ (180°) and $[1a]Ti(CH_2Ph)_2$ (137°). The angles around the oxygen donor are similar in all three structures, as are the sums of the angles at oxygen (332.6 , 343.5 , and 345.1°). The C(1)–Hf–C(2) angle ($104.0(2)^\circ$) is slightly larger than the C–M–C angles in $[1a]ZrMe_2$ and $[1a]Ti(CH_2Ph)_2$. Since the preferred orientation of a 2,6-disubstituted phenyl ring appears to be roughly perpendicular to the MNC_{ipso} plane, a structure of type **A** appears to be more capable of accommodating large substituents in the ortho positions of the aryl ring than a structure of type **B**. However, steric interaction between large ortho substituents and large alkyl groups on the metal in a structure of type **A** appears to lead to a distortion of that structure toward type **B**, even though a type **B** structure may not be possible with the largest ortho substituents on the aryl rings. Therefore, the observed structure of $[1c]HfEt_2$ is the best compromise between type **A** and type **B**, perhaps on the basis of steric interactions alone.

The structural data for $[1a]Ti(CH_2Ph)_2$, $[1a]ZrMe_2$, and $[1c]HfEt_2$, combined with the solution NMR behavior, suggest that the energy differences between structures of type **A** and structures of type **B**, or any variation between **A** and **B**, are not large. Within the oxygen donor system we propose that the structure of type **A** is favored until steric interactions distort it toward a type **B** structure and, if sterically possible, all the way to a type **B** structure.

Synthesis of Zirconium Complexes That Contain [(ArylNCH₂CH₂)₂S]²⁻ Ligands. [(2,6-Me₂C₆H₃-NHCH₂CH₂)₂S] (H₂[**2a**]) and [(2,6-*i*-Pr₂C₆H₃NHCH₂CH₂)₂S] (H₂[**2c**]) can be prepared in two steps, as shown in eq 8. The ditosylate intermediate was formed es-



entially quantitatively and was used without purification in order to minimize the consequences of its apparent slow decomposition. Reaction of the ditosylate with the neat, excess 2,6-disubstituted aniline followed by removal of the unreacted aniline in vacuo gave high yields of H₂[**2a**] and H₂[**2c**]. H₂[**2a**] could be crystallized in 70% yield from cold pentane, while H₂[**2c**] was obtained as a viscous orange oil that could be used without further purification. Dimethylamido, dichloro, and dimethyl complexes ([**2a,c**]Zr(NMe₂)₂, [**2a,c**]ZrCl₂, and [**2a,c**]ZrMe₂) could all be prepared by methods analogous to those shown in eqs 5–7. [**2a**]ZrMe₂ appears to be thermally unstable at room temperature (a solution in benzene changed color from light yellow to dark brown in less than 1 h), while [**2c**]ZrMe₂ is much more stable in solution. [**2c**]Zr(CH₂CHMe₂)₂ is the product (in 46% yield) of the reaction between 2 equiv

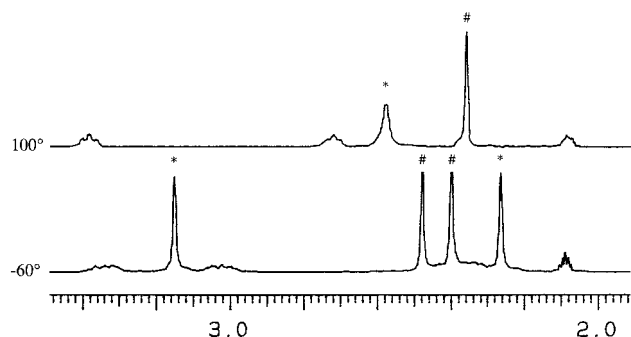


Figure 4. Proton NMR spectra (in toluene- d_8) of $[2a]Zr(NMe_2)_2$ (*, resolved and average resonances for the NMe_2 ligands; #, resolved and average resonances for the methyl groups in the 2,6-dimethylphenylimido ligand).

of $(Me_2CHCH_2)MgCl$ and $[2c]ZrCl_2$; NMR samples of $[2c]Zr(CH_2CHMe_2)_2$ in toluene- d_8 show no signs of decomposition after being heated to 80 °C in the process of recording NMR spectra. We believe that the instability of $[2a]ZrMe_2$ is a consequence of some intermolecular decomposition reaction that is inherently faster for methyl complexes that contain the $[2a]^{2-}$ ligand than for methyl complexes that contain the $[1a]^{2-}$ ligand, while intermolecular decomposition is inherently slower for complexes that contain the bulkier $[2c]^{2-}$ ligand than for complexes that contain the $[2a]^{2-}$ ligand.

A major difference between the sulfur-donor complexes and the oxygen-donor complexes is that type **B** complexes are readily observable in sulfur donor complexes. For example, proton spectra of dimethylamido complexes at -60 °C or below reveal two types of dimethylamido ligands (each containing equivalent methyl groups) and two types of ortho substituents in the 2,6-disubstituted phenylamido ligand, consistent with a "trigonal" structure of type **B** in which rotation about the N-C_{ipso} bond is slow on the NMR time scale. In $[2a]Zr(NMe_2)_2$, for example, the dimethylamido proton resonances are found at 2.26 and 3.15 ppm at -60 °C (Figure 4). Above 60 °C the resonances for the two dimethylamido ligands coalesce to give an average resonance at 2.58 ppm. The ortho methyl group resonances and backbone resonances also coalesce to give resonances consistent with C_{2v} symmetry on the NMR time scale. In the $^{13}C\{^1H\}$ NMR spectrum of $[2a]Zr(NMe_2)_2$ at room temperature a broad amido methyl carbon resonance is observed at 43.3 ppm. It should be noted that there is a dramatic temperature dependence of most resonances over the 160 °C range in the proton NMR spectra shown in Figure 4, with the "average" resonances not appearing at the average chemical shift. Therefore, we believe that over the 160 °C temperature range the temperature-dependent process cannot be described as simply as interconversion of two structures of type **B** via an intermediate of type **A** but as a change in the nature of the average lowest energy conformation itself. As we alluded to in the previous section, the energy differences between various nonideal intermediate structures are small, and over a temperature range of 160 °C the "average" of the distribution could change considerably. Interestingly, rotation about the C_{ipso}-N bond is slow on the NMR time scale even at 100 °C in $[2c]Zr(NMe_2)_2$, where the molecules have a plane of symmetry on the NMR time scale, as evidenced by the observation of two isopropyl

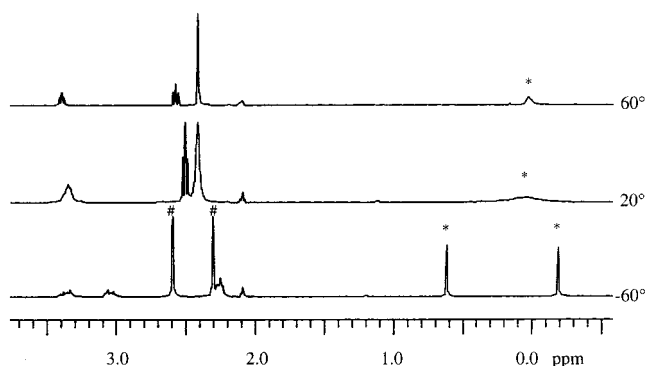


Figure 5. Variable-temperature proton NMR spectra of $[2a]ZrMe_2$ in toluene- d_8 (*, $ZrMe_2$ resonance(s); #, aryl methyl resonances in $[2a]^{2-}$).

methyl resonances in the 2,6-diisopropylphenylimido group. Complexes $[2a,c]ZrCl_2$ appear to contain only a C_2 axis on the basis of four different isopropyl methyl groups being observed in NMR spectra at room temperature. Therefore, we believe that complexes $[2a,c]ZrCl_2$ are dimers containing two bridging chlorides but having no plane of symmetry.

In $[2a]ZrMe_2$ the two zirconium-methyl resonances that are observed at 0.6 and -0.2 ppm at -20 °C or below coalesce at ~7 °C (Figure 5). The average $ZrMe$ resonance is again not found strictly at the average position, as a consequence of temperature-dependent chemical shifts over the 120 °C range. In $[2c]ZrMe_2$ the two zirconium methyl resonances coalesce at ~14 °C. Since ν_0 at the coalescence temperature is not known accurately from these data, we cannot determine the barrier for this rearrangement process accurately. If we do assume the value of ν_0 found at low temperatures, then we find that the rate constants at the coalescence temperature in $[2a]ZrMe_2$ and $[2c]ZrMe_2$ are 530 and 600 s^{-1} , respectively, or $\Delta G^\ddagger \approx 13$ kcal mol^{-1} . In the ^{13}C NMR spectrum of $[2a]Zr(^{13}CH_3)_2$ at -40 °C (in CD_2Cl_2) the two zirconium-methyl carbon resonances are observed at 41.9 and 38.0 ppm, while in $[2c]Zr(^{13}CH_3)_2$ at 0 °C (in toluene- d_8) they are observed at 45.5 and 39.3 ppm.

An X-ray structural study of $[2a]ZrMe_2$ revealed the structure to be closest to type **B** (Tables 1 and 2; Figure 6), on the basis of the angle between the N(1)-Zr-S and N(2)-Zr-S planes being 140° and the S-Zr-C(2) angle being 160.60(9)°. The C(1)-Zr-C(2) angle (101.37(13)°) is again approximately what it is in the other three structures reported here. The Zr-S bond length (2.8046(9) Å) is slightly longer than that reported for zirconium-sulfur dative bonds in $[(t-BuN-o-C_6H_4)_2S]ZrCl(NMe_2)$ (2.7273(10) Å)³⁴ or $[Cp^*_2ZrMe(tht)]^+[BPh_4]^-$ (2.730(4) Å).³⁵ The C(3)-S-C(4) angle (105.0(2)°) is distinctively smaller than the C-O-C angle in the three compounds that contain the oxygen donor (~113°), comparable to the corresponding C-S-C angle of $[(t-BuN-o-C_6H_4)_2S]ZrCl(NMe_2)$ (106.1(2)°).³⁴ The angle at sulfur should be compared to the corresponding angle in titanium complexes that contain the substituted $[(O-o-C_6H_4)_2S]^{2-}$ ligand³⁶⁻⁴⁰ (e.g., 100.8(2)° in $[(O-2,4-Me_2o-C_6H_4)_2S]Ti(O-i-Pr)_2$ ³⁹). It appears that the structure is

(34) Graf, D. D.; Schrock, R. R.; Davis, W. M. Unpublished results.

(35) Eshuis, J. J.; Tan, Y. Y.; Meetsma, A.; Teuben, J. H.; Renkema, J.; Evens, G. G. *Organometallics* **1992**, *11*, 362.

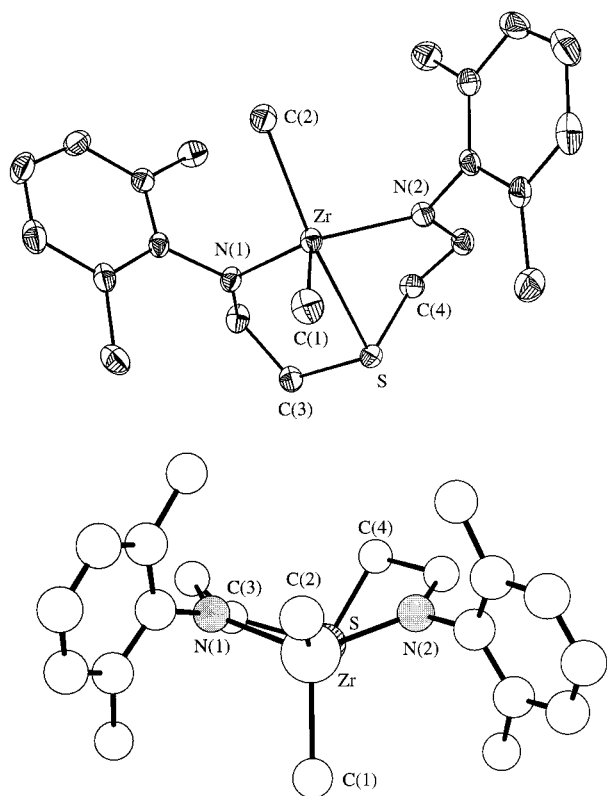


Figure 6. (a, top) ORTEP drawing of the structure of **[2a]**-ZrMe₂. (b, bottom) Top view (Chem 3D) of the structure of **[2a]**-ZrMe₂.

being "held" in approximately a type **B** conformation by the restriction placed on the C–S–C angle. The relatively small alkyl groups on Zr and in the ortho positions of the aryl amido substituents are allowing the molecule to distort toward a structure of type **A**, but the combination of the longer Zr–S bond and the smaller C–S–C angle does not allow the C–S–C unit to "rotate" readily (without changing the C–S–C angle significantly) toward an intermediate in which the angle between the N(1)–Zr–S and N(2)–Zr–S planes is approximately 180° and the N–Zr–N angle is ~140°. It should be noted that the Zr–N–C angles (110.1(2) and 116.4(2)°) are ~4° smaller in **[2a]**-ZrMe₂ than in **[1a]**-ZrMe₂ or **[1c]**-HfEt₂, as if the amido substituents are pushed toward the coordination pocket. At this stage we believe this to be a consequence of the large size of S relative to O, making the MSC₂N ring effectively larger than an MOC₂N ring.

Cationic Alkyl Complexes of Zr and Hf. Addition of 1 equiv of [PhNMe₂H][B(C₆F₅)₄] in C₆D₅X (X = Br, Cl) to **[1a,c]**MMe₂ (M = Zr, Hf) at –30 °C followed by warming to room temperature leads to protonolysis of one of the methyl groups and formation of cationic complexes having a single plane of symmetry that contain coordinated dimethylaniline. The reactions are

(36) Miyatake, T.; Mizunuma, K.; Kakugo, M. *Makromol. Chem.-Macromol. Symp.* **1993**, *66*, 203.

(37) Miyatake, T.; Mizunuma, K.; Seki, Y.; Kakugo, M. *Makromol. Chem.-Rapid Commun.* **1989**, *10*, 349.

(38) Porri, L.; Ripa, A.; Colombo, P.; Miano, E.; Capelli, S.; Meille, S. V. *J. Organomet. Chem.* **1996**, *514*, 213.

(39) Fokken, S.; Spaniol, T. P.; Kang, H.-C.; Massa, W.; Okuda, J. *Organometallics* **1996**, *15*, 5069.

(40) van der Linden, A.; Schaverien, C. J.; Meijboom, N.; Ganter, C.; Orpen, A. G. *J. Am. Chem. Soc.* **1995**, *117*, 3008.

relatively clean according to ¹H NMR spectra. For example, the room-temperature proton NMR spectra of **[1a]**-ZrMe(NMe₂Ph)[B(C₆F₅)₄] and **[1c]**-ZrMe(NMe₂Ph)[B(C₆F₅)₄] are presented in parts a and b, respectively, of Figure 7. Their most important features are the following: (i) four (rather than two) multiplets are observed for the OCH₂CH₂N backbone protons; (ii) broad resonances near 6 ppm and a broadened singlet near 2.7 ppm can be assigned to aromatic protons and the equivalent methyl groups of coordinated *N,N*-dimethylaniline, respectively, in a molecule having a single plane of symmetry; (iii) a singlet at 0.1 to 0.3 ppm integrated as three protons can be ascribed to the zirconium-bound methyl group; (iv) four methyl resonances belonging to the isopropyl groups in the ortho positions of the aryl rings are consistent with no rotation about the N–C_{ipso} bonds. (The two resonances for ortho methyl groups in the zirconium complex whose spectrum is shown in Figure 7a are accidentally coincident at room temperature, but at 40–60 °C two separate singlets of area 6 each are found.) One equivalent of free NMe₂Ph was added to C₆D₅Br solutions of the complexes **[1a,c]**-ZrMe(NMe₂Ph)[B(C₆F₅)₄]. In both cases resonances due to the aromatic protons of free NMe₂Ph (300 and 500 MHz) were distinctly separated from those of bound NMe₂Ph at room temperature. (See, for example, Figure 7a.) For **[1a]**-ZrMe(NMe₂Ph)[B(C₆F₅)₄] resonances due to the NMe groups in free and bound dimethylaniline also were well-separated, while in **[1c]**-ZrMe(NMe₂Ph)[B(C₆F₅)₄] they accidentally overlapped. In the ¹³C{¹H} NMR spectrum (125 MHz) of **[1c]**-ZrMe(NMe₂Ph)[B(C₆F₅)₄] in the presence of 1 equiv of free NMe₂Ph all the resonances belonging to free NMe₂Ph are sharp and located at the expected chemical shifts, while those for bound NMe₂Ph are broad. These results suggest that exchange of free and coordinated NMe₂Ph in **[1c]**-ZrMe(NMe₂Ph)[B(C₆F₅)₄] is slow on the NMR time scale. They also suggest that the broad aromatic resonances for coordinated dimethylaniline in Figure 7a must be attributed to a phenomenon other than dimethylaniline exchange. Most resonances in the spectrum of **[1c]**-HfMe(NMe₂Ph)[B(C₆F₅)₄] at room temperature are not sharp, but at –20 °C the spectrum is analogous to the room-temperature spectrum of **[1c]**-ZrMe(NMe₂Ph)[B(C₆F₅)₄] described above and shown in Figure 7b, with the exception that now two separate methine septet resonances are observed and the resonances belonging to aromatic protons of PhNMe₂ ligand are better resolved. The phenomenon that gives rise to broadened resonances in the Zr and Hf cationic complexes is not known. We propose that it involves some restricted rotation about the N–C_{ipso} bond in bound dimethylaniline and/or some restricted movement within the diamido/donor ligand itself.

All attempts to isolate dimethylaniline adducts in the solid state have not yet been successful. However, addition of excess ether and then pentane to freshly prepared chlorobenzene solutions of **[1a]**-MMe(NMe₂Ph)[B(C₆F₅)₄] (M = Zr, Hf) led to precipitation of **[1a]**-MMe(ether)[B(C₆F₅)₄] (M = Zr, Hf) complexes in high yield in the form of colorless powders. The complexes are poorly soluble in benzene, forming biphasic mixtures. Their NMR spectra in C₆D₅Br are completely analogous to those for the dimethylaniline complexes.

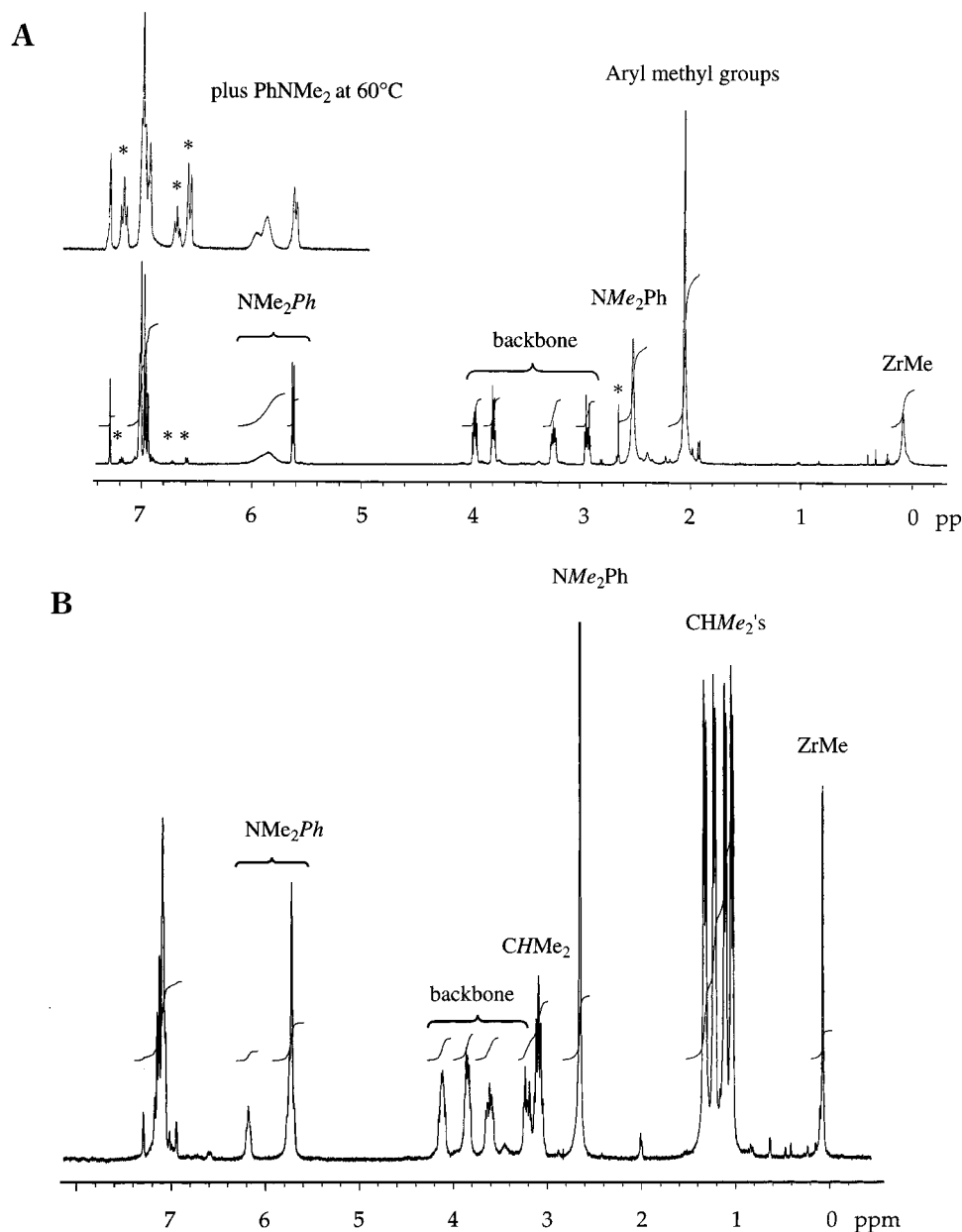


Figure 7. (a, top) Proton NMR spectrum of $\{[1\mathbf{a}]\text{Zr}(\text{NMe}_2\text{Ph})(\text{Me})\}[\text{B}(\text{C}_6\text{F}_5)_4]$ in chlorobenzene- d_5 at 22 °C (*, free PhNMe_2) and at 60 °C in the presence of ~ 1 equiv of added PhNMe_2 . (b, bottom) Proton NMR spectrum of $\{[1\mathbf{c}]\text{Zr}(\text{NMe}_2\text{Ph})(\text{Me})\}[\text{B}(\text{C}_6\text{F}_5)_4]$ in chlorobenzene- d_5 .

The proton spectra contain sharp, well resolved triplet and quartet resonances due to one coordinated ether molecule, and the two ethyl groups are equivalent on the NMR time scale. The resonances for ether that has been added to a sample of $\{[1\mathbf{a}]\text{HfMe}(\text{NMe}_2\text{Ph})\}[\text{B}(\text{C}_6\text{F}_5)_4]$ are found in the expected positions in both the Zr and Hf examples, and free and coordinated ether do not exchange on the NMR time scale at room temperature. The coordinated ether methyl resonances are found at unusually high field (0.21 and 0.17 ppm for the Zr and Hf complexes, respectively) in each case, presumably as a consequence of the ether donor being "sandwiched" between aryl groups at a crowded coordination site. It should be noted that the two types of ortho methyl groups on the aryl ring in $\{[1\mathbf{a}]\text{HfMe}(\text{ether})\}^+$ complexes are inequivalent and do not interconvert readily, consistent with slow rotation about the N–C_{ipso} bond on the NMR time scale. The Zr complex is thermally unstable in solution and in the solid state.

However, at -30 °C in $\text{C}_6\text{D}_5\text{Br}$ it remains virtually unchanged after 1 week. Decomposition of $\{[1\mathbf{a}]\text{ZrMe}(\text{ether})\}[\text{B}(\text{C}_6\text{F}_5)_4]$ in $\text{C}_6\text{D}_5\text{Br}$ at room temperature produces red needles over the course of several hours; this complex is insoluble in common solvents and was not characterized further. (No free ether is detected in the resulting solution.) In contrast, $\{[1\mathbf{a}]\text{HfMe}(\text{ether})\}[\text{B}(\text{C}_6\text{F}_5)_4]$ is thermally stable and can be stored for days at room temperature both as a solid and in solution. All data are consistent with a solvent being bound relatively strongly to hafnium compared to zirconium and with decomposition of a four-coordinate cationic species formed upon loss of the solvent donor from the five-coordinate solvent adduct.

Addition of $[\text{PhNMe}_2\text{H}][\text{B}(\text{C}_6\text{F}_5)_4]$ to $[2\mathbf{a}]\text{ZrMe}_2$ in either chlorobenzene- d_5 or bromobenzene- d_5 in the presence of THF results in the clean formation of the THF-stabilized species $\{[2\mathbf{a}]\text{ZrMe}(\text{THF})_x\}[\text{B}(\text{C}_6\text{F}_5)_4]$ and free dimethylaniline. In this species the zirconium

methyl resonance is observed at 0.2 ppm and the two aryl methyl resonances are seen at 2.20 and 1.89 ppm. On the basis of the formation of only monosolvated cations containing ether or dimethylaniline in the oxygen donor system, we believe that most likely $x = 1$. When the same reaction is carried out in chlorobenzene- d_5 in the absence of THF, a relatively clean proton NMR spectrum is obtained at room temperature, consistent with formation of $\{[2a]ZrMe(PhNMe_2)\}[B(C_6F_5)_4]$, in which the methyl resonance is found at 0.43 ppm. Similar results were found for the complexes obtained upon addition of $[PhNMe_2H][B(C_6F_5)_4]$ to $[2c]ZrMe_2$. However, the cations in the sulfur donor system do not appear to be formed as cleanly and do not appear to be as stable as those generated in the oxygen donor system.

At this stage we have not been able to observe monomethyl Zr and Hf cations generated with $[Ph_3C][B(C_6F_5)_4]$ in chlorobenzene or bromobenzene, perhaps as a consequence of the poor donating ability of bromobenzene or chlorobenzene or the unexpected complexity of the NMR spectra. (Cationic methyl species generated in chlorobenzene with $[Ph_3C][B(C_6F_5)_4]$ are effective initiators for 1-hexene polymerization, as described below; thus, we assume that they are formed and do not decompose readily to a significant extent.) We also have not been able to observe monomethyl cations, even dimethylaniline adducts, that contain Ti.

Polymerization of 1-Hexene. Addition of 25 equiv of 1-hexene to an NMR mixture of $[1a]TiR_2$ ($R = Me, CH_2Ph$) and $[PhNMe_2H][B(C_6F_5)_4]$ in C_6D_5Br results in only short-term polymerization activity. Some monomer is not consumed. New olefinic resonances appear that are centered around δ 5.3 ppm, which suggests that β -hydride elimination accompanies decomposition of $\{[1a]TiR\}^+$. Use of $[Ph_3C][B(C_6F_5)_4]$ as an initiator led to immediate decomposition and formation of dark oily precipitates.

In contrast, complexes $[1a-d]MMe_2$ ($M = Zr, Hf$), when activated with $[Ph_3C][B(C_6F_5)_4]$ in chlorobenzene, were found to be efficient initiators for polymerization of 1-hexene. The temperature was kept at 0 °C in order to minimize decomposition that would result from a significant exotherm. Data can be found in Table 3. The low value of dn/dc for poly(1-hexene) in dichloromethane limited the accuracy of the molecular weight data (see Experimental Section), so only broad trends will be discussed. We will first discuss systems that contain oxygen donor ligands and will assume complete activation and a quantitative yield of initiator before 1-hexene is added. To provide a basis for comparison most of the comments will be based on a theory concerning base lability. (In reactions initiated with $[Ph_3C][B(C_6F_5)_4]$ it will be assumed that the C_6D_5Cl solvent is functioning as the base, as that it is likely to be more labile than dimethylaniline.) We will not discuss polydispersity, as the polydispersity values are not accurate beyond two significant figures. Several poly(1-hexene) samples were examined by ^{13}C NMR and found to be atactic.

(i) Initiator. Run 17 (compared with run 1) provides evidence in the form of a relatively low yield of poly(1-hexene) (in 1 h reaction time) that $\{[1a]ZrMe(PhNMe_2)\}^+$ is a slower catalyst than $\{[1a]ZrMe(PhCl)\}^+$. Runs 5 and 18 confirm that trend and are consistent with the expected stronger binding of dimethylaniline

Table 3. GPC and Yield Data for Poly(1-hexene) Using Zr or Hf Precursors Activated with $[Ph_3C][B(C_6F_5)_4]$ (A) or $[PhNMe_2H][B(C_6F_5)_4]$ (B)^a

no.	complex/activator	M_n (theory)	M_n^g	M_w^g	M_w/M_n	% yield
1	[1a]ZrMe ₂ /A	16 800	11 700	18 000	1.6	100
2	[1b]ZrMe ₂ /A	16 800	9 200	11 100	1.2	94
3	[1c]ZrMe ₂ /A	16 800	2 500	4 00	1.7	96
4	[1a]HfMe ₂ /A	16 800	18 100	24 700	1.4	94
5	[1b]HfMe ₂ /A	16 800	17 500	20 500	1.2	95
6		16 800	17 600	24 000	1.3	100
7		25 200	25 400	31 700	1.3	100
8		25 200 ^b	21 200	28 700	1.4	98
9		33 600	21 200	26 800	1.3	100
10		33 600 ^c	24 600	30 600	1.3	100
11		33 600 ^d	24 600	31 700	1.3	97
12		33 600 ^e	20 400	28 000	1.4	96
13	[1c]HfMe ₂ /A	16 800	7 200	9 700	1.3	99
14		25 200	7 500	10 200	1.4	100
15		33 600	6 000	8 300	1.4	100
16	[1d]HfMe ₂ /A	16 800	3 800	6 300	1.6	77
17	[1a]ZrMe ₂ /B	16 800	9 000	13 000	1.4	70
18	[1b]HfMe ₂ /B	16 800	23 000	32 600	1.4	21
19	[2a]ZrMe ₂ /A ^a	16 800	16 000	18 400	1.2	86
20	(3 h) ^a	16 800	15 900	18 400	1.2	100
21	a	25 200	20 900	25 000	1.2	
22	(3 h) ^a	25 200	19 100	23 000	1.2	100
23	[2a]ZrMe ₂ /B	16 800 ^f	16 900	23 200	1.4	94
24		16 800 ^f	16 900	22 600	1.3	96
25	[2a]ZrMe ₂ /B (5 h)	21 880	20 800	24 500	1.2	94
26		25 200 ^f	16 900	22 500	1.3	88
27		33 600 ^f	19 400	28 700	1.5	84
28		33 600 ^f	20 700	30 900	1.5	87
29		50 400 ^f	28 400	36 100	1.3	77
30	[2c]ZrMe ₂ /B	16 800 ^f	4 300	5 500	1.3	75
31		16 800 ^f	6 100	8 200	1.4	85
32	[2c]Zr(CH ₂ CHMe ₂) ₂ /B	16 800 ^f	4 200	6 800	1.6	82
33	[2c]Zr(CH ₂ CHMe ₂) ₂ /B	16 800 ^f	4 300	6 400	1.5	80

^a Conditions: 0.040 mmol of the metal complex and activator, 0 °C, 10 mL of chlorobenzene, 1 h, unless otherwise noted.

^b Conditions: 0.025 mmol of the metal complex, 0.022 mmol of the activator, 6.60 mmol of the monomer. ^c Conditions: 0.017 mmol of the metal complex, 0.015 mmol of the activator, 6.00 mmol of the monomer. ^d Conditions 0.012 mmol of the metal complex, 0.008 mmol of the activator, 3.20 mmol of the monomer. ^e The monomer was added in two 200 equiv portions with 25 min interval, total experiment time 1 h 15 min. ^f Conditions: 50 μ mol of the catalyst, 50 μ mol of the activator, 13 mL of chlorobenzene, 3 h at 0 °C. ^g Determined by GPC on-line light scattering (Wyatt Technology).

to Hf versus Zr. The molecular weight is also higher than theory based on equivalents of monomers added, which could be attributed to a significantly stronger binding of base to the initiating species versus the propagating species.

(ii) Aryl Group. For Zr catalysts increasing the steric bulk of the aryl groups (runs 1–3) leads to formation of shorter polymers, although polymer yields are uniformly high. Therefore, after termination of a given chain, a new chain can be initiated without significant catalyst decomposition; i.e., the process is a chain transfer. These results are consistent with a greater lability of the base as the size of the substituents on the aryl ring increase, with consequently a more competitive chain transfer process. These results suggest that at least for 1-hexene under the conditions we have employed, the olefin does not add rapidly enough to the four-coordinate cation to compete with chain transfer.

A similar trend is observed for hafnium (runs 4, 5, and 13). Polymer yields are again high, but polymers shorter than expected are found only in run 13. Mo-

lecular weights are again somewhat higher than expected in runs 4 and 5. We propose that hafnium yields higher molecular weight poly(1-hexene) as a consequence of the base being bound more strongly, thereby preventing β -hydride elimination in a four-coordinate base-free cation. A large k_p/k_t ratio would also contribute to a larger than expected molecular weight that would counteract the consequences of β -hydride elimination. Although the rate of polymerization would be expected to be slower for hafnium than for zirconium, run 13 (unlike run 18) evidently is complete in 1 h at 0 °C and the yield of poly(1-hexene) is high, presumably since the "base" in this case is a more labile chlorobenzene.

Use of [**1d**]HfMe₂ leads to the formation of a relatively low molecular weight polymer in 77% yield (entry 16). In an analogous polymerization using 50 equiv of 1-hexene in C₆D₅Br at 0 °C and followed by proton NMR, olefinic proton resonances were observed as a broad singlet centered at δ 5.4 ppm. If we assume that these olefinic resonances arise from vinylidene end groups in the poly(1-hexene), then we can conclude that β -hydride elimination is minimized when 2,6-disubstituted aryl groups are employed. One ortho substituent can block only one side of a structure of type **A**, leaving the other side relatively accessible for β -hydride elimination.

(iii) Amount of Monomer. We chose to examine the result of varying the amount of monomer with [**1b**]-HfMe₂ as the catalyst precursor and [Ph₃C][B(C₆F₅)₄] as the activator, since this combination proved to be relatively well-behaved in the experiments at the scale of 200 equiv of 1-hexene (entries 5 and 6). The results obtained are summarized in entries 5–12. Under standard conditions (see Experimental Section), increasing the amount of 1-hexene from 200 (entries 5 and 6) to 300 equiv (entry 7) produced a higher molecular weight in proportion to the amount of additional monomer employed. Lowering the catalyst concentration from 0.040 to 0.022 mmol/10 mL produced a similar result (entry 8). However, increasing the amount of the monomer to 400 equiv in experiments where catalyst concentrations of 0.040, 0.015, and 0.008 mmol/10 mL were employed (entries 9–11), or adding the monomer in two equal portions (entry 12), did *not* lead to a proportional increase in the molecular weight. An analogous trend is observed for complexes that contain [**1c**]²⁻, although at much lower molecular weight levels (entries 13–15), as noted earlier. We conclude that there is a limit to the polymer chain length as a consequence of β -hydride elimination under the conditions employed.

The proposal that a five-coordinate cation must lose a base in order to react with 1-hexene is supported by the finding that neither {[**1c**]ZrMe(ether)}[B(C₆F₅)₄] nor {[**1c**]HfMe(ether)}[B(C₆F₅)₄] will initiate the polymerization of 1-hexene in C₆D₅Br at room temperature; no change is observed after 1 h. Moreover, neither compound initiates the polymerization of ethylene at 1 atm and 25 °C. Therefore, even ethylene cannot attack the five-coordinate base adduct to produce a pseudooctahedral intermediate. These results also make it clear that diethyl ether essentially does not dissociate from the

metal, while dimethylaniline, and especially chlorobenzene, are relatively labile.

Similar trends were observed for catalytic reactions that employ the sulfur donor ligands. A comparison of runs 1, 19, and 20 suggest that the [**2a**]ZrMe₂/A initiator is slower than the [**1a**]ZrMe₂/A initiator but that β -hydride elimination does not seem to be as rapid in the sulfur donor ligand system. In fact, run 20 is reminiscent of run 5 or 6. Use of the [**2a**]ZrMe₂/B as the initiator again leads to shorter poly(1-hexene) chains, as β -hydride elimination again becomes more competitive with chain growth, and approximately the same limitation to polymer chain length (20 000 to 25 000). The results using [**2c**]Zr(CH₂CHMe₂)₂/B as an initiator (runs 32 and 33) are the same as the results of runs 30 and 31, which suggests that higher alkyl complexes can be activated successfully. So far the data are not indicative of any dramatic instability of the cations formed in the sulfur system. However, qualitative evidence suggests that the rates of polymerization are slightly slower in the sulfur donor system than in the oxygen donor system.

Discussion

Although group 4 amido complexes that contain a bis-(trimethylsilyl)amido ligand have been known for some time,^{41–43} group 4 amido ligands that do not contain a silyl substituent and that are multidentate are relatively recent additions to the area of early-transition-metal amido chemistry. Although trimethylsilyl substituents add a significant amount of steric bulk to an amido ligand and also create an amido ligand that has suitable electronic characteristics for binding to an early transition metal, silyl substituents are prone to hydrolysis or to CH activation.⁴³ Monodentate amido ligands also can be displaced from the coordination sphere, either as an anion (rarely) or upon protonation or alkylation. The combination of one aryl and one alkyl (*tert*-butyl) substituent in an amido ligand has recently been employed to considerable advantage in early-transition-metal chemistry, especially the chemistry of molybdenum.^{44–49} Therefore, the tridentate diamido/donor ligands of the type reported here are attractive candidates for a variety of chemistry involving relatively reactive metal centers. They are related to diamido/donor ligands of the type [(*t*-BuN-*o*-C₆H₄)₂O]²⁻ reported recently,^{11,12} in that the amido nitrogens are bound to both an alkyl and to an aryl substituent. However, the *tert*-butyl groups in the [(*t*-BuN-*o*-C₆H₄)₂O]²⁻ ligands probably create a significantly greater degree of steric

(41) Andersen, R. A. *Inorg. Chem.* **1979**, *18*, 2928.

(42) Andersen, R. A. *J. Organomet. Chem.* **1980**, *192*, 189.

(43) Planalp, R. P.; Andersen, R. A.; Zalkin, A. *Organometallics* **1983**, *2*, 16.

(44) Stokes, S. L.; Davis, W. M.; Odom, A. L.; Cummins, C. C. *Organometallics* **1996**, *15*, 4521.

(45) Peters, J. C.; Odom, A. L.; Cummins, C. C. *Chem. Commun.* **1997**, 1995.

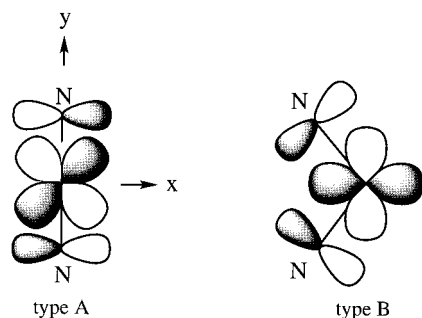
(46) Laplaza, C. E.; Johnson, M. J. A.; Peters, J. C.; Odom, A. L.; Kim, E.; Cummins, C. C.; George, G. N.; Pickering, I. J. *J. Am. Chem. Soc.* **1996**, *118*, 8623.

(47) Johnson, M. J. A.; Odom, A. L.; Cummins, C. C. *Chem. Commun.* **1997**, 1523.

(48) Johnson, M. J. A.; Lee, P. M.; Odom, A. L.; Davis, W. M.; Cummins, C. C. *Angew. Chem., Int. Ed. Engl.* **1997**, *36*, 87.

(49) Fickes, M. G.; Odom, A. L.; Cummins, C. C. *Chem. Commun.* **1997**, 1993.

Chart 1



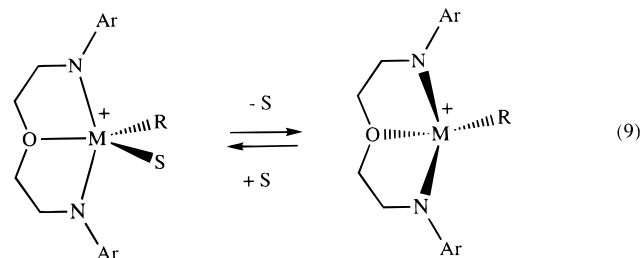
congestion in complexes that contain that ligand than in the complexes reported here, and the phenylene backbone is not likely to be as flexible as in the ligands reported here. As a consequence of the relatively flexible backbone in the ligands reported here, the donor atom *could* dissociate from the metal and, after rotation about the C–donor bonds, actually turn away from the metal. However, we believe that dissociation of an O or S donor, especially in cationic complexes, is not taking place to any significant degree, at least for Zr and Hf, where metal–ligand bond strengths are relatively high compared to Ti–donor bond strengths. However, we cannot be certain that a donor never dissociates from the metal, especially in some neutral complexes, and especially in complexes in which the bond strength is relatively low (Ti).

An important issue in amido complexes in general is the degree of π bonding between the amido nitrogen and the metal. In the diamido/donor ligands reported here the aryl substituent is generally turned 90° from where it should be for maximum conjugation of the aryl π system with the nitrogen lone pair. Therefore, the lone pair on nitrogen is likely to be involved primarily in π bonding to the metal. However, the amount of π bonding in the two structures (type **A** and type **B**) should be roughly the same. The major π -bonding interaction in the structure of type **A** is that between the unsymmetric combination of p orbitals on the two amido nitrogens and the d_{xy} orbital (in the coordinate system shown in Chart 1), while in the structure of type **B** it is that between the symmetric combination of p orbitals on the two amido nitrogens and the $d_{x^2-y^2}$ orbital. (The N–M–N system is viewed from a position trans to the donor in both type **A** and type **B** structures.) In the structure of type **B** the donor in the axial position cannot π bond to a significant degree with the metal. In contrast, an sp^2 -hybridized donor in a structure of type **A** *could* be involved in π bonding to the metal to some degree through the d_{xz} orbital. However, planarity or near-planarity of the donor in a structure of type **A** alone is not evidence for a significant degree of π bonding, since the electron density could be centered largely on the donor in a p orbital, especially in the case of a relatively electronegative oxygen atom donor. If only one significant π bond is invoked in an electron-counting scheme, all neutral dialkyl complexes or cationic monoalkyl complexes (that contain an additional external σ donor) of either type **A** or type **B** are 12-electron species. Therefore, there does not seem to be any significant electronic (π bonding) advantage to a structure of type **A** compared to one of type **B** or to any intermediate version between A and B. This

prediction is consistent with the fact that the structures of dialkyl complexes found here can be rationalized on the basis of steric arguments alone.

The low electron count for dialkyl complexes would seem to contribute to their instability with respect to β -hydride elimination or abstraction reactions. Some hafnocene monoalkyl⁵⁰ and dialkyl complexes⁵¹ have been isolated where the alkyl contains a β -proton, and stable Zr or Hf diamido dialkyl complexes have been known for some time.^{41–43} Therefore, the stability of some of the neutral Zr and Hf species reported here is not a complete surprise. It is beginning to appear that diamido group 4 dialkyl complexes can be relatively stable toward β -elimination, with the stability increasing significantly in the order Ti < Zr < Hf. Nevertheless, the relatively high stability of zirconium and hafnium *cationic* alkyl intermediates in polymerization reactions reported here was surprising to us, especially in view of the relatively low electron count (assuming one M–N π bond). The instability of the analogous cationic titanium alkyl complexes was closer to the expected behavior. It should be pointed out, however, that the mode of decomposition of no neutral or cationic alkyl complex reported here has been elucidated, and therefore we should not presume that the mechanism of decomposition is uniform or that the diamido/donor ligand is never involved.

All evidence at this time suggests that 12e monosolvated monoalkyl complexes (for convenience of type **A** shown in eq 9) must lose a base to yield a 10e four-coordinate cation. This four-coordinate cation most



likely has a core geometry that is as close as possible to a pseudotetrahedron; i.e., the axial amido nitrogens in the type **A** structure most likely would move toward the position occupied by the base as the base leaves the coordination sphere (eq 9). This movement is the same as that which leads to a conversion of a type **A** structure to a type **B** structure. In a five-coordinate structure of type **B**, in which the base is in an axial position, formation of the four-coordinate pseudo-tetrahedral species would require (after loss of S) only some relatively small movement of the R group. A pseudotetrahedral structure is a sensible and accessible geometry for a d^0 complex and contrasts markedly with the distorted-trigonal geometry of a typical cationic metallocene monoalkyl complex that is believed to be formed upon activating group 4 metallocene dialkyl complexes. Formation of inactive monosolvated $[Cp_2MR(S)]^+$ species (M = Zr, Hf) and required loss of solvent in order to generate catalytically active species

(50) Guo, Z.; Swenson, D. C.; Jordan, R. F. *Organometallics* **1994**, *13*, 1424.

(51) Erker, G.; Schlund, R.; Krüger, C. *Organometallics* **1989**, *8*, 2349.

have been amply demonstrated.^{50,52,53} If we assume for the moment that decomposition of intermediate four-coordinate cations is of the same type for all three metals and that a base protects against that decomposition by forming a five-coordinate adduct, then all of the behavior we have seen so far in these systems can be explained. We are ready to modify this viewpoint as more data become available.

The results reported here should be contrasted with those of McConville and co-workers, where Ti catalysts supported by (ArylNCH₂CH₂CH₂NAryl)²⁻ ligands (e.g., Ar = 2,6-*i*-Pr₂C₆H₃) are found to yield poly(1-hexene) in a living manner in the presence of excess 1-hexene.⁶⁻⁹ As the 1-hexene is depleted, a decomposition step involving the anion competes with polymerization and destroys the catalyst.⁹ The reason the titanium complexes prepared and studied here are not relatively well-behaved polymerization catalysts for 1-hexene, while Ti[ArylNCH₂CH₂CH₂NAryl]₂ compounds yield systems that are living for the polymerization of 1-hexene in the presence of excess 1-hexene, is not known. Interestingly, there has been no report of [ArylNCH₂CH₂CH₂NAryl]²⁻ zirconium or hafnium catalysts behaving in a living manner as 1-hexene polymerization catalysts, and although relatively rigid diamido/donor systems based on 2,6-disubstituted pyridine have been prepared for both Ti and Zr,^{21,23} no polymerization activity was reported. It should be noted that the number of group 4 diamido or diamido/donor systems in which no N-Si bond is present is still small and they have not yet been explored in detail as polymerization catalysts, so it is perhaps too early to attempt to rationalize results obtained in different systems at this stage.

The studies reported here should be regarded as only an outline. The nature of the base, the size of the alkyl in both the five-coordinate adducts and four-coordinate cations that contain the growing polymer chain, the reactivity of the monomer, the degree of base labilization in five-coordinate cations, and the protection against β -hydride elimination afforded by the ortho substituents or structures of type **B** are all important features of polymerization reactions that remain to be fully explored.

Conclusions

Titanium, zirconium, and hafnium dialkyl complexes that contain diamido/donor ligands of the general formula (ArylNHCH₂CH₂)₂O can be prepared readily. Dimethyl complexes can be activated by protonation or oxidative cleavage of the alkyl to yield cationic species, many of which can be observed for Zr and Hf, especially when an oxygen donor such as diethyl ether is bound to the metal. If the base is sufficiently labile (dimethylaniline or chlorobenzene), then 1-hexene can be polymerized relatively efficiently. The vast majority of the results can be explained in terms of a required loss of a coordinated base (solvent) from a five-coordinate base adduct and subsequent olefin attack on a four-coordinate cationic intermediate. β -Hydride elimination is proposed to occur in a four-coordinate cationic intermediate. Hafnium systems (activated with [Ph₃C][B(C₆F₅)₄])

were found to behave best in the sense that the molecular weight of poly(1-hexene) is approximately equal to the amount of monomer employed, and the polydispersity is relatively low. β -Hydride elimination becomes an important factor in polymers that contain more than 300 equiv of monomer and limits the molecular weight to \sim 25 000. Dialkylzirconium complexes that contain a [(ArylNHCH₂CH₂)₂S]²⁻ ligand, as well as cationic complexes, appear to be less stable than analogous [(ArylNHCH₂CH₂)₂O]²⁻ complexes. Nevertheless, cationic complexes that contain the sulfur donor ligand behave like complexes that contain the oxygen donor ligand in the studies conducted so far.

Experimental Section

General Procedures. All experiments were performed under a nitrogen atmosphere in a Vacuum Atmospheres drybox or by standard Schlenk techniques unless otherwise specified. Tetrahydrofuran and diethyl ether were sparged with nitrogen and passed through two columns of activated alumina. Toluene was distilled from sodium/benzophenone. Pentane was sparged with nitrogen, then passed through one column of activated alumina, and then passed through another of activated Q5. Chlorobenzene was distilled from CaH₂ under nitrogen. All solvents were stored in the drybox over 4 Å molecular sieves. 1-Hexene was refluxed over sodium for 4 days, distilled, and stored over 4 Å sieves.

NMR data were recorded at 500 or 300 MHz (¹H), 75 or 125 MHz (¹³C), and 470 MHz (¹⁹F). Chemical shifts are listed in parts per million downfield from tetramethylsilane or CFCl₃ (for ¹⁹F), unless specified otherwise. A standard variable-temperature unit was used to control the probe temperature in variable temperature runs, and temperatures are considered accurate to \pm 1 °C. NMR solvents were sparged with nitrogen and stored over 4 Å molecular sieves. Elemental analyses were performed by Microlytics of Deerfield, MA. Chloride analysis was performed by Schwarzkopf Microanalytical Laboratory, Inc., of Woodside, NY. X-ray data were collected on a Siemens SMART/CCD diffractometer.

All gel permeation chromatography (GPC) experiments were carried out using two Jordi-Gel DVB Mixed Bed columns in series, a Wyatt Mini Dawn light scattering detector operating at 690 nm, and a Knauer refractometer. Solutions of samples dissolved in CH₂Cl₂ were filtered through a Millex-SR 0.5 μ m filter. All GPC data were analyzed using Astrette 1.2 (Wyatt Technology). Values of dn/dc were obtained under the assumption that all sample eluted from the column and were averaged for various runs. The low value of dn/dc (the change in refractive index versus concentration) for poly(1-hexene) in dichloromethane limited the accuracy of the molecular weight data obtained via light scattering.

Zr(NMe₂)₄, Hf(NMe₂)₄, and Ti(CH₂Ph)₄ were prepared according to the literature procedure. [Ph₃C][B(C₆F₅)₄] and [PhNMe₂H][B(C₆F₅)₄] were provided by Exxon Chemicals. 2,2'-Thiodiethanol, 2,6-Dimethylaniline, 2,6-diethylaniline, 2,6-diisopropylaniline, and 2-*tert*-butylaniline were purchased from Aldrich.

Preparation of Compounds. H₂[1a]. Solid (TsOCH₂CH₂)₂O (6.47 g, 15.6 mmol) was added to a chilled (-30 °C) solution of LiNH(2,6-Me₂C₆H₃) (4.0 g, 31.5 mmol) in THF (40 mL). The reaction mixture was stirred at room temperature for 72 h, and all volatile components were then removed in vacuo. The residue was extracted with pentane, and the extract was concentrated in vacuo until white crystals appeared. Recrystallization at -30 °C from pentane afforded colorless crystals (3.0 g, 9.6 mmol, 62%): ¹H NMR δ 2.24 (s, 12, ArMe), 2.95 (dt, 4, CH₂N), 3.15 (t, 4, OCH₂), 3.50 (t, 2, NH), [6.88 (dd, 2), 6.99 (d, 2) (H_{ary})]; ¹³C{¹H} NMR δ 18.9 (ArMe), 48.6 (CH₂N), 70.8 (OCH₂), [122.7, 129.6, 130.2, 146.8] (C_{ary}).

(52) Jordan, R. F. *Adv. Organomet. Chem.* **1991**, *32*, 325.

(53) Wu, Z.; Jordan, R. F. *J. Am. Chem. Soc.* **1995**, *117*, 5867.

Anal. Calcd for $C_{20}H_{28}N_2O$: C, 76.88; H, 9.03; N, 8.97. Found: C, 76.93; H, 8.96; N, 8.83.

H₂[1b]. LiNH(2,6-Et₂C₆H₃) (3.44 g, 22.2 mmol) was added in two portions to a chilled (−30 °C) solution of 4.59 g (11.1 mmol) of (TsOCH₂CH₂)₂O in 80 mL of THF. The resulting yellow solution was warmed slowly to room temperature and was stirred for 30 h. The solvent was removed in vacuo, and the resulting viscous solid was extracted with two 30 mL portions of pentane. Removal of the pentane from the filtered extract in vacuo yielded 3.4 g of a slightly yellow oil. Most of the 1-(2,6-diethylphenyl)morpholine side product of the reaction was distilled away from the product at 40–50 °C/200 mTorr to yield 2.5 g (52%) of an orange oil which was shown by NMR to be the 90% (by mass) pure H₂[1b]: ¹H NMR δ 1.21 (d, 12, ArCH₂CH₃), 2.69 (q, 8, ArCH₂CH₃), 3.00 (t, 4, OCH₂), 3.27 (t, 4, CH₂N), 3.60 (br t, 2, NH), 6.98–7.08 (m, 6, H_{aryl}); ¹³C{¹H} NMR δ 15.14 (CH₂CH₃), 24.76 (CH₂CH₃), 49.93 (CH₂N), 70.67 (OCH₂), [123.25, 127.13, 136.80, 145.29] (C_{aryl}). It was used without further purification.

H₂[1c]. Solid (TsOCH₂CH₂)₂O (5 g, 12.0 mmol) was added to a chilled (−30 °C) solution of LiNH(2,6-*i*-Pr₂C₆H₃) (4.53 g, 24.8 mmol) in THF (30 mL). The reaction mixture was stirred at room temperature for 24 h, and all volatile components were removed in vacuo. The residue was extracted with pentane, and the extract was filtered. Removal of all volatile components in vacuo gave an orange oil (4.2 g, 82%), which was used without further purification. Upon standing, the oil would crystallize in some cases. An analytically pure sample was obtained by recrystallization from a concentrated pentane solution at −30 °C: ¹H NMR δ 1.06 (d, 24, CHMe₂), 3.07 (q, 4, CH₂N), 3.35 (t, 4, OCH₂), 3.48 (heptet, 4, CHMe₂), 3.60 (t, 2, NH), 7.18–7.14 (m, 6, H_{aryl}); ¹H NMR (CDCl₃) δ 1.27 (d, 24, CHMe₂), 3.14 (br t, 4, CH₂N), 3.36 (heptet, 4, CHMe₂), 3.57 (br, 2, NH), 3.70 (t, 4, OCH₂), 7.05–7.18 (m, 6, H_{aryl}); ¹³C{¹H} NMR (CDCl₃) δ 24.3 (CHMe₂), 27.6 (CHMe₂), 51.3 (CH₂N), 70.7 (OCH₂), [123.6, 123.7, 142.5, 142.9] (C_{aryl}). Anal. Calcd for C₂₈H₄₄N₂O: C, 79.19; H, 10.44; N, 6.60. Found: C, 79.14; H, 10.23; N, 6.30.

H₂[1d]. To a solution of 8.96 g (60 mmol) of 2-*t*-BuC₆H₄NH₂ in 150 mL of THF precooled to −30 °C was added in two portions over 15 min 24 mL of 2.5 M solution of BuLi in hexanes (60 mmol). The reaction mixture was stirred for 40 min more after which to the resulting yellowish solution of LiNH(2-*t*-BuC₆H₄) was quickly added at room temperature 6.65 g (60 mmol) of Me₃SiCl. The color was immediately discharged, and a white precipitate formed. The mixture was stirred for an additional 40 min, after which the liquid phase was filtered from the precipitate. The solvent was removed in vacuo, and the resulting oil was reextracted into pentane to completely remove the remaining amount of LiCl. The extract was filtered and evacuated to yield 13.25 g (99%) of NH(SiMe₃)(2-*t*-BuC₆H₄) as a yellowish oil: ¹H NMR (CDCl₃) δ 0.32 (s, 9, SiMe₃), 1.44 (s, 9, CMe₃), 3.70 (br s, 1, NH), [6.73 (td, 1), 6.78 (dd, 1), 7.09, (td, 1), 7.27 (dd, 1)] (H_{aryl}).

To a precooled (−30 °C) solution of 13.25 g (60 mmol) of NH(SiMe₃)(2-*t*-BuC₆H₄) in 100 mL of THF was added in three portions over a period of 1 h 24 mL of a 2.5 M solution of butyllithium in hexane (60 mmol). After 2 h 100 mL of THF was added, the mixture was cooled again to −30 °C, and 12.43 g (30 mmol) of solid (TsOCH₂CH₂)₂O was added over a period of 10 min. The reaction mixture was stirred for 12 h at room temperature, and the greenish solution was separated from a white precipitate by filtration. The filtrate was concentrated in vacuo until it became viscous. The oil was extracted with two portions of pentane (70 mL each), and the extracts were taken to dryness in vacuo to yield 11.0 g of an almost colorless oil that was shown by NMR to be a mixture of NHSiMe₃(2-*t*-BuC₆H₄) and [(SiMe₃)(2-*t*-BuC₆H₄)NCH₂CH₂]₂O in about a 1:2 molar ratio. NHSiMe₃(2-*t*-BuC₆H₄) (2.8 g) was removed by distillation in vacuo (46 °C/170 mTorr) to leave 7.8 g (50.7%) of [(SiMe₃)(2-*t*-BuC₆H₄)NCH₂CH₂]₂O: ¹H NMR (CDCl₃) δ [0.07

(s), 0.08 (s)] (18, SiMe₃), [1.41 (s), 1.42 (s)] (18, CMe₃), [3.07 (m, 2), 3.31 (overlapped m, 6)] (OCH₂CH₂N), [6.90 (m, 2), 7.02 (m, 2), 7.10 (m, 2), 7.45 (dt, 2)] (H_{aryl}); ¹³C{¹H} NMR δ 0.78 (SiMe₃), 33.06 (CMe₃), 36.43 (CMe₃), 51.91 (CH₂N), 69.95 (OCH₂), [125.29, 125.91, 129.96, 133.90, 146.65, 148.16] (C_{aryl}).

A solution of 10.6 g (20.7 mmol) of [(SiMe₃)(2-*t*-BuC₆H₄)NCH₂CH₂]₂O in 100 mL of ether was stirred at 40 °C with 200 mL of 3 N HCl for 13 h. The reaction mixture was treated with 3 N KOH until basic. The organic phase was separated, and the aqueous phase was extracted with an additional 100 mL of ether. The extracts were combined, washed with water until neutral, and dried over anhydrous Na₂SO₄. Removal of the ether in vacuo yielded 7.33 g (96%) of H₂[1d] as a rose-colored oil which solidified after 2 days. An analytically pure sample in the form of almost colorless crystals was obtained by recrystallization from pentane at −30 °C: ¹H NMR (CDCl₃) δ 1.45 (s, 18, CMe₃), 3.41 (t, 4, CH₂N), 3.85 (t, 4, OCH₂), 4.4 (vbr s, 2, NH), [6.75 (m, 4), 7.18 (td, 2), 7.29 (dd, 2)] (H_{aryl}); ¹³C{¹H} NMR (CDCl₃) δ 30.08 (CMe₃), 34.36 (CMe₃), 44.31 (CH₂N), 69.61 (OCH₂), [112.25, 117.53, 126.46, 127.30, 134.02, 146.57] (C_{aryl}). Anal. Calcd for C₂₄H₃₆N₂O: C, 78.21; H, 9.85; N, 7.60. Found: C, 78.24; H, 10.08; N, 7.54.

[1a]TiCl₂. A hexane solution of butyllithium (0.8 mL of 2.5 M, 2.0 mmol) was added to a solution of 312 mg (1.0 mmol) of H₂[1a] in 10 mL of ether at −30 °C. The mixture was warmed to room temperature. After 40 min the reaction mixture was again cooled to −30 °C and a suspension of TiCl₄(THF)₂ (334 mg, 1.0 mmol) was added to the stirred mixture. The color of the mixture changed immediately to deep red, and a red-brown precipitate was formed. The mixture was stirred for 1 h at room temperature, and solvents were then removed in vacuo. The dry residue was extracted with methylene chloride, the extract was filtered, and the solvent was removed in vacuo to yield brick red [1a]TiCl₂; yield 244 mg (56.9%): ¹H NMR δ 2.42 (s, 12, ArMe), 3.27 (t, 4, CH₂N), 3.65 (t, 4, OCH₂), 6.94–7.20 (m, 6, H_{aryl}); ¹³C{¹H} NMR δ 19.18 (ArMe), 59.35 (CH₂N), 72.33 (OCH₂), [126.79, 129.06, 131.33, 155.85] (C_{aryl}). Anal. Calcd for C₂₀H₂₆Cl₂N₂O: C, 55.97; H, 6.11; N, 6.53. Found: C, 55.51; H, 6.25; N, 6.23.

[1a]TiMe₂. A 3.0 M solution of MeMgCl in THF (0.33 mL) was added to a cold (−30 °C) stirred suspension of 200 mg (0.47 mmol) of [1a]TiCl₂ in 6 mL of ether. The color of the mixture changed immediately to brown. The mixture was stirred for 35 min at room temperature, and the solvent was removed in vacuo. The residue was extracted with 15 mL of pentane. The extract was filtered and taken to dryness in vacuo to yield 95 mg (52.5%) of pure [1a]TiMe₂ in a form of a yellow powder: ¹H NMR δ 0.90 (s, 6, TiMe), [2.508 (s, 6), 2.509 (s, 6H)] (ArMe), 3.36 (m, 8, OCH₂CH₂N), [7.01 (m, 2), 7.14 (m, 4)] (H_{aryl}); ¹³C{¹H} NMR δ 19.17 (ArMe), 57.03 (CH₂N), 60.75 (TiMe), 70.67 (OCH₂), [125.39, 128.99, 131.76, 152.92] (C_{aryl}).

[1a]Ti(CH₂Ph)₂. (a) From Ti(CH₂Ph)₄. To a red solution of 824 mg (2.0 mmol) of TiBz₄ in 10 mL of pentane was added a solution of 624 mg (2.0 mmol) in 5 mL of pentane. The reaction mixture was stirred for 40 h, and all volatile components of the mixture were then removed in vacuo, leaving an oily dark red residue. This residue was washed with 7 mL of pentane and then 10 mL of ether. The remaining red-orange precipitate was isolated and dried in vacuo; yield 165 mg (15%). Red needles suitable for an X-ray structure determination were grown from a concentrated benzene-*d*₆ solution at room temperature: ¹H NMR δ 2.43 (br s, 12, ArMe), 2.66 (br s, 4, TiCH₂Ph), 2.99 (t, 4, CH₂N), 3.31 (t, 4, OCH₂), [6.56 (br s, 4), 6.81 (t, 2), 7.02 (m), 7.12 (d), 10] (H_{aryl}); ¹³C{¹H} NMR δ 19.71 (ArMe), 58.07 (CH₂N), 70.65 (OCH₂), [121.75, 125.72, 126.11, 127.81, 129.35, 133.49, 150.01, 154.96] (C_{aryl}). The resonances due to the benzylic carbons that are not observed at room temperature appear in the spectrum measured at 65 °C (125 MHz) at 91.7 ppm (v br). Anal. Calcd for C₃₄H₄₀N₂O: C, 75.54; H, 7.46; N, 5.18. Found: C, 73.90; H, 7.05; N, 4.80.

(b) From [1a]TiCl₂ and Benzyl Grignard Reagent. A 1.0 M solution of PhCH₂MgCl in ether (0.47 mL) was added to a stirred suspension of 100 mg (0.23 mmol) of [1a]TiCl₂ in 3 mL of ether. The suspension quickly turned dark red. The mixture was stirred for 25 min at room temperature, and the solvent was removed in vacuo. The residue was washed with two portions of pentane (5 mL each) and extracted with methylene chloride. The extract was filtered, and the solvent was removed in vacuo. The dark red solid was washed with pentane; yield 72 mg of crude product. The crude product was washed with minimal cold ether to give the pure product as a red-orange powder; yield 44 mg (35%).

[1a]Zr(NMe₂)₂. A solution of Zr(NMe₂)₄ (1.07 g, 4.0 mmol) in pentane (4 mL) was added to a solution of H₂[1a] (1.26 g, 4.05 mmol) in pentane (14 mL) at room temperature. Crystals formed upon mixing. After 12 h the crystals were isolated by filtration and the mother liquor was cooled to -30 °C to yield a second crop; total yield 1.90 g (97%): ¹H NMR δ 2.43 (s, 12, ArMe), 2.65 (s, 12, ZrNMe₂), 3.21 (t, 4, CH₂N), 3.55 (t, 4, OCH₂), [6.92 (t, 2), 7.11 (d, 4)] (H_{aryl}); ¹³C{¹H} NMR δ 19.6 (ArMe), 42.1 (ZrNMe₂), 54.1 (CH₂N), 72.8 (OCH₂), [123.7, 128.9, 134.9, 152.7] (C_{aryl}). Anal. Calcd for C₃₂H₅₄N₄OZr: C, 58.85; H, 7.82; N, 11.44. Found: C, 59.16; H, 7.95; N, 11.46.

[1a]ZrCl₂. Neat Me₃SiCl (5.2 g, 48 mmol) was added to a solution of [1a]Zr(NMe₂)₂ (1.17 g, 2.39 mmol) in 80 mL of diethyl ether at room temperature. The solutions were mixed thoroughly. After 46 h colorless needles (0.99 g) were isolated by filtration (88% yield). Using less solvent led to cocrystallization of intermediate [1a]Zr(NMe₂)Cl with the desired product: ¹H NMR δ 2.43 (s, 12, ArMe), 3.09 (t, 4, CH₂N), 3.49 (t, 4, OCH₂), [6.94 (dd, 2), 7.01 (d, 4)] (H_{aryl}); ¹H NMR (CD₂-Cl₂) δ 2.43 (s, 12, ArMe), 3.77 (t, 4, CH₂N), 4.62 (t, 4, OCH₂), [7.01 (dd, 2), 7.10 (d, 4)] (H_{aryl}); ¹³C{¹H} NMR δ 19.4 (ArMe), 55.8 (CH₂N), 73.8 (OCH₂), [126.7, 129.7, 134.6, 148.5] (C_{aryl}). Anal. Calcd for C₂₀H₂₆Cl₂N₂OZr: C, 50.83; H, 5.55; N, 5.93. Found: C, 50.83; H, 5.57; N, 5.84.

[1a]ZrMe₂. A chilled (-30 °C) solution of MeMgBr (3.0 M in ether, 0.580 mL, 1.74 mmol) was added to a suspension of [1a]ZrCl₂ (400 mg, 0.85 mmol) in CH₂Cl₂ (10 mL) at -30 °C. After the mixture was stirred for 20 min at room temperature, dioxane (159 mg, 1.80 mmol) was added. After 20 min of additional stirring, the reaction mixture was filtered. Upon addition of pentane (5 mL) the filtrate turned slightly cloudy and was filtered again. All volatile components were then removed from the filtrate. The residue was dissolved in ether, and the solution was cooled to -30 °C to yield 252 mg (69%) of colorless cubes in two crops. Crystals suitable for X-ray crystallography were obtained by crystallization from ether at -30 °C: ¹H NMR δ 0.27 (s, 6, ZrMe), 2.44 (s, 12, ArMe), 3.27 (m, 8, OCH₂CH₂N), [7.01 (dd, 2), 7.14 (d, 4)] (H_{aryl}); ¹³C{¹H} NMR δ 19.3 (ArMe), 43.4 (ZrMe), 55.5 (CH₂N), 74.7 (OCH₂), [125.7, 129.4, 136.5, 148.7] (C_{aryl}). Anal. Calcd for C₂₂H₃₂N₂OZr: C, 61.21; H, 7.47; N, 6.49. Found: C, 61.31; H, 7.56; N, 6.46.

[1a]Zr(CH₂CMe₃)Cl. A chilled (-30 °C) solution of BrMgCH₂-CMe₃ (3.16 M in ether, 0.236 mL, 0.74 mmol) was added to a suspension of [1a]ZrCl₂ (160 mg, 0.34 mmol) in CH₂Cl₂ (8 mL) at -30 °C. A fine precipitate formed, and after the mixture was stirred for 30 min at room temperature, dioxane (70 mg, 1.80 mmol) was added. After 20 min the reaction mixture was filtered. All volatile components were removed from the filtrate, and the residue was dissolved in ether and filtered again. The ether solution was cooled to -30 °C to yield 42 mg (24%) of colorless crystals in two crops: ¹H NMR δ 1.11 (s, 9, CH₂CMe₃), 1.23 (s, 2, ZrCH₂), 2.46 (s, 6, ArMe), 2.50 (s, 6, ArMe), 3.16 (m, 4, CH₂N), 3.37 (m, 2, OCH₂C), 3.50 (m, 2, OCH₂C), [6.97 (t, 2), 7.08 (d, 4)] (H_{aryl}); ¹³C{¹H} NMR δ [19.8, 20.0] (ArMe), 35.0 (CH₂CMe₃), 35.8 (CH₂CMe₃), 55.5 (CH₂N), 73.4 (OCH₂), 81.4 (ZrCH₂), [126.1, 129.52, 129.55, 135.05, 135.14, 149.8] (C_{aryl}). Anal. Calcd for C₂₅H₃₇ClN₂OZr: C, 59.08; H, 7.34; N, 5.51. Found: C, 59.14; H, 7.42; N, 5.46.

[1a]Zr(CH₂CMe₃)₂. A solution of LiCH₂CMe₃ (68 mg, 0.87 mmol) in ether (2 mL) was added to a suspension of [1a]ZrCl₂ (200 mg, 0.42 mmol) in ether (6 mL) at -30 °C. [1a]ZrCl₂ dissolved immediately, and a fine precipitate of LiCl formed rapidly. After 15 min the product was isolated by crystallization from ether at -30 °C to yield 146 mg (63%) of colorless crystals in two crops: ¹H NMR δ 0.91 (s, 4, ZrCH₂CMe₃), 0.99 (s, 18, ZrCH₂CMe₃), 2.53 (s, 12, ArMe), 3.26 (t, 4, CH₂N), 3.43 (t, 4, OCH₂C), [6.96 (t, 2), 7.11 (d, 4)] (H_{aryl}); ¹³C{¹H} NMR δ 20.3 (ArMe), 35.0 (CH₂CMe₃), 36.5 (CH₂CMe₃), 55.7 (CH₂N), 73.4 (OCH₂), 89.1 (ZrCH₂), [125.4, 129.5, 135.1, 152.3] (C_{aryl}). Anal. Calcd for C₃₀H₄₈N₂OZr: C, 66.24; H, 8.89; N, 5.15. Found: C, 66.17; H, 8.55; N, 4.98.

[1a]Hf(NMe₂)₂. A solution of 2.50 g (7.06 mmol) of Hf(NMe₂)₄ in 5 mL of pentane was added at room temperature to a solution of 2.19 g (7.02 mmol) of H₂[1a] in 35 mL of pentane. After 40 min all volatile components of the reaction mixture were removed in vacuo to leave analytically pure [1a]-Hf(NMe₂)₂ as a white powder; yield 3.91 g (96%): ¹H NMR δ 2.45 (s, 12, ArMe), 2.69 (s, 12, HfNMe₂), 3.25 (t, 4, CH₂N), 3.52 (t, 4, OCH₂), [6.90 (t, 2), 7.12 (d, 4)] (H_{aryl}); ¹³C{¹H} NMR δ 19.14 (ArMe), 41.54 (HfNMe₂), 53.88 (CH₂N), 72.61 (OCH₂), [123.39, 128.46, 134.90, 152.52] (C_{aryl}). Anal. Calcd for C₂₂H₃₈-ON₄Hf: C, 49.95; H, 6.64; N, 9.71. Found: C, 50.01; H, 6.27; N, 9.50.

[1a]HfCl₂. To a solution of 2.02 g (3.5 mmol) of [1a]Hf(NMe₂)₂ in 80 mL of ether at room temperature was added 3.80 g (35 mmol) of Me₃SiCl. After 4 days the reaction mixture was taken to dryness in vacuo and the white residue was washed twice with 10 mL portions of ether and dried in vacuo to afford 1.85 g (94%) of analytically pure [1a]HfCl₂ as a colorless powder: ¹H NMR δ 2.46 (s, 12, ArMe), 3.19 (t, 4, CH₂N), 3.47 (t, 4, OCH₂), [6.94 (m, 2), 7.04 (d, 4)] (H_{aryl}); ¹³C{¹H} NMR δ 19.06 (ArMe), 54.82 (CH₂N), 73.87 (OCH₂), [125.86, 129.21, 134.65, 149.06] (C_{aryl}). Anal. Calcd for C₂₀H₂₆-Cl₂N₂OHf: C, 42.91; H, 4.68; N, 5.00. Found: C, 42.82; H, 4.33; N, 4.90.

[1a]HfMe₂. To a stirred suspension of 1.73 g (3.09 mmol) of [1a]HfCl₂ in 50 mL of ether was added 2.15 mL of a 3.0 M solution of MeMgCl in THF. After 50 min at room temperature the reaction mixture was filtered and the white residue was washed with an additional 30 mL of ether. The ether fractions were combined, filtered through Celite, and evaporated to dryness in vacuo to yield crude [1a]HfMe₂. Analytically pure product was obtained in 78% yield as a colorless powder by recrystallization from CH₂Cl₂/Et₂O (1:1) mixtures at -30 °C: ¹H NMR δ 0.06 (s, 6, HfMe), 2.46 (s, 12, ArMe), 3.31 (m, 8, OCH₂CH₂N), [6.98 (t, 2), 7.12 (d, 4)] (H_{aryl}); ¹³C{¹H} NMR δ 18.95 (ArMe), 53.74 (HfMe), 55.07 (CH₂N), 73.88 (OCH₂), [125.02, 128.99, 135.96, 148.86] (C_{aryl}). Anal. Calcd for C₂₂H₃₂N₂O: C, 50.91; H, 6.21; N, 5.40. Found: C, 50.48; H, 6.32; N, 5.40.

[1a]Hf(CH₂CHMe₂)₂. To a stirred suspension of 0.84 g (1.5 mmol) of [1a]HfCl₂ in 30 mL of ether was added 1.5 mL of a 2.0 M solution of ClMgCH₂CHMe₂ in THF. After 1 h the mixture was filtered, and the ether was removed from the filtrate in vacuo to give 895 mg (99%) of [1a]Hf(CH₂CHMe₂)₂ as a colorless powder pure by NMR: ¹H NMR δ 0.51 (d, 4, HfCH₂), 0.95 (d, 12, CHMe₂), 2.01 (heptet, 2, CHMe₂), 2.56 (s, 12, ArMe), 3.36 (m, 8, OCH₂CH₂N), [7.01 (m, 2), 7.16 (m, 4)] (H_{aryl}); ¹³C{¹H} NMR δ 19.29 (ArMe), 29.08 (CHMe₂), 30.16 (CHMe₂), 55.18 (CH₂N), 73.12 (OCH₂), 88.31 (HfCH₂), [124.93, 129.04, 135.44, 150.06] (C_{aryl}).

[1b]TiCl₂. Preparation of this complex was completely analogous to that of [1a]TiCl₂ from 758 mg of the 90% (by mass) pure H₂[1b] (1.86 mmol), 1.49 mL of 2.5 M solution of BuLi (3.73 mmol), and 623 mg (1.86 mmol) of TiCl₄(THF)₂. The isolated yield of red [1b]TiCl₂ was 346 mg (38%): ¹H NMR δ 1.32 (t, 12, ArCH₂Me), [2.75 (A wing of AB q of q), 3.05 (B wing of AB q of q), 8] (ArCH₂Me), 3.35 (t, 4, CH₂N), 3.70 (t, 4, OCH₂), 7.09 (pseudo s, 6, H_{aryl}); ¹³C{¹H} NMR δ 15.22

(ArCH₂Me), 24.27 (ArCH₂Me), 61.06 (CH₂N), 72.17 (OCH₂), [126.45, 127.15, 136.64, 155.10] (C_{aryl}).

[1b]TiMe₂. To a stirred suspension of 243 mg (0.5 mmol) of **[1b]TiCl₂** in 9 mL of ether was added 0.34 mL of a 3.0 M solution of MeMgCl in THF. The greenish mixture was stirred for 1 h at room temperature. The solvent was removed in vacuo. Pentane (10 mL) was added to the residue, and the mixture stood at -30 °C. After 2 h the precipitate was isolated and dried in vacuo to yield 85 mg (38%) of pure **[1b]TiMe₂** in a form of a yellow-brown powder: ¹H NMR δ 0.89 (s, 6, TiMe), 1.32 (t, 12, ArCH₂Me), 3.01 (q, 8, ArCH₂Me), 3.34 (t, 4, CH₂N), 3.45 (t, 4, OCH₂), 7.10–7.21 (m, 6, H_{aryl}); ¹³C{¹H} NMR δ 15.81 (ArCH₂Me), 24.46 (ArCH₂Me), 58.82 (CH₂N), 61.14 (TiMe), 70.64 (OCH₂), [125.83, 126.56, 139.32, 151.92] (C_{aryl}).

[1b]Zr(NMe₂)₂ and **[1b]Hf(NMe₂)₂**. These complexes were prepared on a 2 mmol scale from a solution of H₂[**1b**] in 4 mL of pentane and M(NMe₂)₄ (M = Zr, Hf) in 4 mL of pentane. After 1 h all volatile components were removed in vacuo leaving the desired complexes in quantitative yields and of sufficient purity for further purposes. The Zr compound was isolated as a slightly yellowish oil which solidified in the freezer. The Hf analogue was formed as a colorless solid.

[1b]Zr(NMe₂)₂: ¹H NMR δ 1.32 (t, 12, ArCH₂Me), 2.88 (m, 8, ArCH₂Me), 2.61 (s, 12, ZrNMe₂), 3.25 (t, 4, CH₂N), 3.57 (t, 4, OCH₂), [7.04 (dd, 2), 7.15 (d), 4] (H_{aryl}); ¹³C{¹H} NMR δ 15.81 (ArCH₂Me), 24.51 (ArCH₂Me), 41.75 (ZrNMe₂), 55.60 (CH₂N), 72.26 (OCH₂), [123.91, 126.00, 140.41, 151.24] (C_{aryl}).

[1b]Hf(NMe₂)₂: ¹H NMR δ 1.32 (t, 12, ArCH₂Me), [2.85 (A wing of AB q of q), 2.99 (B wing of AB q of q), 8] (ArCH₂Me), 2.66 (s, 12, HfNMe₂), 3.28 (t, 4, CH₂N), 3.52 (t, 4, OCH₂), [7.04 (dd, 2), 7.16 (d), 4] (H_{aryl}); ¹³C{¹H} NMR δ 15.83 (ArCH₂Me), 24.44 (ArCH₂Me), 41.60 (HfNMe₂), 55.66 (CH₂N), 72.44 (OCH₂), [123.92, 125.94, 140.67, 151.44] (C_{aryl}).

[1b]ZrCl₂ and **[1b]HfCl₂**. These two compounds were prepared on a 2 mmol scale from **[1b]M(NMe₂)₂** (M = Zr, Hf) in 7 mL of ether and 20 equiv of Me₃SiCl. After 14 h the crystalline products were filtered off, washed with two portions of pentane (3 mL each), and dried in vacuo. The isolated yields were 88% for **[1b]ZrCl₂** and 83% for **[1b]HfCl₂**.

[1b]ZrCl₂: ¹H NMR δ 1.33 (t, 12, ArCH₂Me), [2.81 (A wing of AB q of q), 3.02 (B wing of AB q of q), 8] (ArCH₂Me), 3.17 (t, 4, CH₂N), 3.57 (t, 4, OCH₂), 7.10 (pseudo s, 6, H_{aryl}); ¹³C{¹H} NMR δ 15.54 (ArCH₂Me), 24.48 (ArCH₂Me), 57.26 (CH₂N), 73.28 (OCH₂), [126.70, 126.73, 139.70, 147.28] (C_{aryl}).

[1b]HfCl₂: ¹H NMR δ 1.34 (t, 12, ArCH₂Me), [2.86 (A wing of AB q of q), 3.04 (B wing of AB q of q), 8] (ArCH₂Me), 3.25 (t, 4, CH₂N), 3.49 (t, 4, OCH₂), 7.04–7.14 (m, 6, H_{aryl}); ¹³C{¹H} NMR δ 15.63 (ArCH₂Me), 24.42 (ArCH₂Me), 55.65 (CH₂N), 73.57 (OCH₂), [126.24, 126.65, 140.04, 148.15] (C_{aryl}).

[1b]ZrMe₂ and **[1b]HfMe₂**. The procedures for the syntheses of these two complexes were identical. To a suspension of 1.4 mmol of **[1b]MCl₂** (M = Zr, Hf) in 12 mL of ether was added 0.95 mL of a 3.0 M solution of MeMgCl in THF. After 1 h the solvent was removed in vacuo and the resulting solid was washed with 3 mL of cold (-30 °C) pentane and dried to yield **[1b]ZrMe₂** (88%, pale beige powder) or **[1b]HfMe₂** (93%, colorless powder), respectively.

[1b]ZrMe₂: ¹H NMR δ 0.21 (s, 6, ZrMe), 1.27 (t, 12, ArCH₂Me), 2.93 (symm 10-line m, 8, ArCH₂Me), 3.34 (m, 8, OCH₂CH₂N), 7.09–7.19 (m, 6, H_{aryl}); ¹³C{¹H} NMR δ 16.11 (ArCH₂Me), 24.65 (ArCH₂Me), 42.96 (ZrMe), 56.88 (CH₂N), 74.01 (OCH₂), [125.80, 126.64, 141.83, 147.07] (C_{aryl}).

[1b]HfMe₂: ¹H NMR δ 0.05 (s, 6, HfMe), 1.29 (t, 12, ArCH₂Me), 2.96 (m, 8, ArCH₂Me), 3.34 (pseudo s, 8, OCH₂CH₂N), 7.08–7.18 (m, 6, H_{aryl}); ¹³C{¹H} NMR δ 16.05 (ArCH₂Me), 24.52 (ArCH₂Me), 53.60 (HfMe), 56.86 (CH₂N), 73.55 (OCH₂), [125.50, 126.59, 141.57, 147.72] (C_{aryl}). Anal. Calcd for C₂₆H₄₀N₂O: C, 54.30; H, 7.01; N, 4.87. Found: C, 53.90; H, 7.38; N, 4.87.

[1c]Zr(NMe₂)₂. A solution of Zr(NMe₂)₄ (2.5 g, 9.4 mmol) in pentane (4 mL) was added to a solution of H₂[**1c**] (4.0 g, 9.4

mmol) in pentane (14 mL) at room temperature. Crystals formed immediately. After the mixture stood overnight, the crystals were collected and the mother liquor was cooled to -30 °C to yield a second crop; total yield 3.85 g (68%): ¹H NMR δ 1.28 (d, 12, CHMe₂), 1.31 (d, 12, CHMe₂), 2.56 (s, 12, ZrNMe₂), 3.33 (t, 4, CH₂N), 3.56 (t, 4, OCH₂), 3.71 (heptet, 4, CHMe₂), 7.05–7.18 (m, 6, H_{aryl}); ¹³C{¹H} NMR δ 25.0 (CHMe₂), 27.0 (CHMe₂), 28.6 (CHMe₂), 42.7 (ZrNMe₂), 57.7 (CH₂N), 72.8 (OCH₂), [124.2, 125.2, 146.2, 150.2] (C_{aryl}). Anal. Calcd for C₃₂H₅₄N₄OZr: C, 63.84; H, 9.04; N, 9.31. Found: C, 63.96; H, 9.16; N, 9.20.

[1c]ZrCl₂. Neat Me₃SiCl (578 mg, 5.3 mmol) was added to a solution of **[1c]Zr(NMe₂)₂** (400 mg, 0.664 mmol) in 10 mL of diethyl ether at room temperature. The solutions were mixed thoroughly by shaking, and the reaction mixture was allowed to stand overnight at room temperature to yield colorless crystals (285 mg; 73% yield). If the reaction mixture is too concentrated, **[1c]Zr(NMe₂)Cl** will cocrystallize with **[1c]ZrCl₂**:

¹H NMR δ 1.26 (d, 12, CHMe₂), 1.51 (d, 12, CHMe₂), 3.35 (t, 4, CH₂N), 3.66 (t, 4, OCH₂), 3.73 (heptet, 4, CHMe₂), 7.17 (br, 6, H_{aryl}); ¹³C{¹H} NMR δ 25.4 (CHMe₂), 26.9 (CHMe₂), 29.0 (CHMe₂), 59.3 (CH₂N), 73.6 (OCH₂), [125.1, 127.6, 145.1, 146.4] (C_{aryl}). Anal. Calcd for C₂₈H₄₂Cl₂N₂OZr: C, 57.51; H, 7.24; N, 4.79. Found: C, 57.10; H, 7.28; N, 4.46.

[1c]ZrMe₂. A chilled (-30 °C) solution of MeMgBr (4.1 M in ether, 0.428 mL, 1.75 mmol) was added to a suspension of **[1c]ZrCl₂** (500 mg, 0.85 mmol) in diethyl ether (20 mL) at -30 °C. A fine precipitate slowly replaced the suspension of crystals, and after the mixture was stirred for 2 h at room temperature, dioxane (154 mg, 1.75 mmol) was added. After an additional 20 min all volatile components were removed and the residue was extracted with pentane. Recrystallization from pentane yielded 280 mg (61%) of colorless crystals: ¹H NMR δ 0.30 (s, 6, ZrMe), 1.23 (d, 12, CHMe₂), 1.38 (d, 12, CHMe₂), 3.41 (br, 8, OCH₂CH₂N), 3.84 (heptet, 4, CHMe₂), 7.12 (br, 6, H_{aryl}); ¹³C{¹H} NMR δ 24.9 (CHMe₂), 27.3 (CHMe₂), 28.9 (CHMe₂), 43.6 (ZrMe), 58.6 (CH₂N), 73.6 (OCH₂), [124.7, 126.5, 146.5, 147.1] (C_{aryl}). Anal. Calcd for C₃₀H₄₈N₂OZr: C, 66.24; H, 8.89; N, 5.15. Found: C, 66.32; H, 8.87; N, 5.12.

[1c]Zr(CH₂CHMe₂)₂. A chilled (-30 °C) solution of BrMgCH₂CHMe₂ (2.51 M in ether, 0.286 mL, 0.72 mmol) was added to a suspension of **[1c]ZrCl₂** (205 mg, 0.35 mmol) in diethyl ether (10 mL) at -30 °C. A fine precipitate slowly replaced the suspension of crystals, and after the solution was stirred for 1.5 h at room temperature, dioxane (63 mg, 0.72 mmol) was added. After 20 min all volatile components were removed in vacuo and the residue was recrystallized from pentane to yield 158 mg (72%) of colorless crystals: ¹H NMR δ 0.70 (d, 4, ZrCH₂), 0.85 (d, 12, CH₂CHMe₂), 1.23 (d, 12, CHMe₂), 1.45 (d, 12, CHMe₂), 1.92 (heptet, 2, CH₂CHMe₂), 3.42 (br, 8, OCH₂CH₂N), 3.91 (heptet, 4, CHMe₂), 7.12–7.15 (br, 6, H_{aryl}); ¹³C{¹H} NMR δ 24.6 (CHMe₂), 27.4 (CHMe₂), 28.4 (CH₂CHMe₂), 28.9 (CHMe₂), 29.7 (CH₂CHMe₂), 58.3 (CH₂N), 74.5 (OCH₂), 78.1 (ZrCH₂), [124.6, 126.2, 146.0, 149.2] (C_{aryl}). Anal. Calcd for C₃₆H₆₀N₂OZr: C, 68.84; H, 9.63; N, 4.46. Found: C, 68.96; H, 9.59; N, 4.40.

[1c]Hf(NMe₂)₂. A solution of Hf(NMe₂)₄ (833 mg, 2.35 mmol) in 3.5 mL of pentane was added to a solution of 1.0 g (2.35 mmol) of H₂[**1c**] in 3.5 mL of pentane at room temperature. After 20 min crystallization of the product began. The reaction was allowed to proceed for 12 h, after which colorless blocks were isolated and washed with cold pentane. Cooling of the mother liquor to -30 °C yielded a second crop; total yield 1.21 g (74.7%): ¹H NMR δ 1.31 (d, 12, CHMe₂), 1.35 (d, 12, CHMe₂), 2.65 (s, 12, HfNMe₂), 3.39 (t, 4, CH₂N), 3.53 (t, 4, OCH₂), 3.78 (heptet, 4, CHMe₂), 7.09–7.21 (m, 6, H_{aryl}); ¹³C{¹H} NMR δ 24.64 (CHMe₂), 26.67 (CHMe₂), 28.09 (CHMe₂), 42.26 (HfNMe₂), 57.39 (CH₂N), 72.49 (OCH₂), [123.79, 124.76, 145.99, 150.12] (C_{aryl}). Anal. Calcd for C₃₂H₅₄N₄O: C, 55.76; H, 7.90; N, 8.13. Found: C, 55.33; H, 7.90; N, 7.87.

[1c]HfCl₂. Me₃SiCl (1.67 g, 15.4 mmol) was added to a

solution of 1.06 g (1.54 mmol) of **[1c]Hf(NMe₂)₂** in 25 mL of ether. After 1 day the vial was shaken to induce crystallization. A fine white precipitate formed immediately. After several hours it was isolated by filtration and washed with pentane. The mother liquor was cooled to -30 °C to yield a second crop; total yield 940 mg (90.5%): ¹H NMR δ 1.28 (d, 12, CHMe₂), 1.49 (d, 12, CHMe₂), 3.41 (t, 4, CH₂N), 3.57 (t, 4, OCH₂), 3.77 (heptet, 4, CHMe₂), 7.15 (br s, 6, H_{aryl}); ¹³C{¹H} NMR δ 25.28 (CHMe₂), 26.65 (CHMe₂), 28.67 (CHMe₂), 58.51 (CH₂N), 73.62 (OCH₂), [124.66, 126.76, 145.08, 146.61] (C_{aryl}). Satisfactory elemental analyses could not be obtained on this compound (low in C).

[1c]HfMe₂. MeMgCl in THF (0.78 mL of a 3.0 M solution) was added to a stirred suspension of 753 mg (1.12 mmol) of **[1c]HfCl₂** in 12 mL of ether. The reaction mixture was stirred for an additional 4 h and filtered. The solvent was removed from the filtrate in vacuo, and the residue was extracted with minimal ether. The extract was filtered, and the ether was removed in vacuo to give 575 mg (81.3%) of pure **[1c]HfMe₂** in the form of a colorless powder: ¹H NMR δ 0.17 (s, 6, HfMe), 1.28 (d, 12, CHMe₂), 1.42 (d, 12, CHMe₂), 3.43 (m, 8, OCH₂CH₂N), 3.90 (heptet, 4, CHMe₂), 7.18 (br s, 6, H_{aryl}); ¹³C{¹H} NMR δ 24.95 (CHMe₂), 26.98 (CHMe₂), 28.58 (CHMe₂), 53.90 (HfMe), 58.33 (CH₂N), 73.55 (OCH₂), [124.29, 125.90, 146.05, 147.18] (C_{aryl}). Satisfactory elemental analyses could not be obtained on this compound (low in C).

[1c]HfEt₂. EtMgBr (0.117 mL of a 3.0 M ether solution, 0.35 mmol, 2.05 equiv) was added to a suspension of 115 mg (0.171 mmol) of **[1c]HfCl₂** in 7 mL of ether. A colorless solution formed almost immediately. After 1.5 h all the volatile components were removed in vacuo and the resulting residue was extracted with pentane. The extract was filtered and evacuated to dryness to yield crude **[1c]HfEt₂**. Recrystallization from pentane at -30 °C gave colorless needles (80 mg, 74%) suitable for X-ray analysis: ¹H NMR δ 0.50 (q, 4, HfCH₂), 1.28 (t, 6, CH₂Me), 1.28 (d, 12, CHMe₂), 1.44 (d, 12, CHMe₂), 3.40 (m, 4, CH₂N), 3.49 (m, 4, OCH₂), 3.89 (heptet, 4, CHMe₂), 7.16–7.22 (m, 6, H_{aryl}); ¹³C{¹H} NMR δ 12.04 (CH₂Me), 24.29 (CHMe₂), 27.11 (CHMe₂), 28.44 (CHMe₂), 58.16 (CH₂N), 66.33 (HfCH₂), 73.52 (OCH₂), [124.16, 125.76, 146.21, 147.71] (C_{aryl}).

(TsOCH₂CH₂)₂S. A slurry of pulverized KOH flakes (3.96 g, 70.6 mmol) in THF (15 mL) was added to a solution of (HOCH₂CH₂)₂S (2 mL, 20 mmol) in THF (10 mL). The reaction mixture was stirred vigorously at room temperature for 1 h and then cooled to 0 °C. A solution of tosyl chloride (7.63 g, 40 mmol) in THF (25 mL) was added dropwise to the chilled mixture over the course of 1 h. The reaction mixture was stirred vigorously at 0 °C for 24 h and filtered. The filtrate was then dried over anhydrous MgSO₄ and the solvent was removed in vacuo to give a viscous pale yellow oil in essentially quantitative yield which would sometimes crystallize upon standing. No further characterization or purification of this compound has been undertaken due to its apparent decomposition in the solid state, even at 0 °C: ¹H NMR (CDCl₃) δ 7.80 (d, 4, H_{aryl}), 7.37 (d, 4, H_{aryl}), 4.10 (t, 4, OCH₂), 2.74 (t, 4, CH₂S), 2.47 (s, 6, CH₃).

[(2,6-Me₂C₆H₃)NHCH₂CH₂]₂S (H₂[2a]). Neat H₂N(2,6-Me₂C₆H₃) (14.78 mL, 120 mmol) was added to (TsOCH₂CH₂)₂S (approximately 20 mmol), and the resulting viscous yellow solution was stirred at 50 °C for 24 h. After several hours at 50 °C, a white precipitate was observed. After 24 h, a solution of NaOH (10 g, 250 mmol) in water (30 mL) was added to the reaction mixture. After 30 min the mixture was extracted with several portions of diethyl ether. The ether layers were combined and dried over anhydrous MgSO₄, and the ether was removed in vacuo. The resulting yellow oil was heated in vacuo (80 °C, 300 mTorr) in order to remove any excess H₂N(2,6-Me₂C₆H₃). The remaining viscous orange oil was dissolved in pentane and the solution stood at 0 °C to yield pale peach crystals in 70% yield overall (from the diol): ¹H NMR δ 6.96 (d, 4, H_m), 6.86 (t, 2, H_p), 3.21 (br s, 2, NH), 2.90 (t, 4, NCH₂),

2.31 (t, 4, CH₂S), 2.18 (s, 12, ArMe); ¹³C{¹H} NMR δ 146.3 (C_{ipso}), 130.0 (C_o), 129.6 (C_m), 122.8 (C_p), 47.6 (NHCH₂), 33.3 (CH₂S), 19.3 (ArMe). Anal. Calcd for C₂₀H₂₈N₂S: C, 73.12; H, 8.59; N, 8.53. Found: C, 73.19; H, 8.55; N, 8.48.

[(2,6-i-Pr₂C₆H₃)NHCH₂CH₂]₂S (H₂[2c]). Neat 2,6-i-Pr₂C₆H₃-NH₂ (22.63 mL, 120 mmol) was added to (TsOCH₂CH₂)₂S (approximately 20 mmol), and the resulting viscous yellow solution was stirred at 50 °C for 24 h. After several hours at 50 °C, a white precipitate was observed. After 24 h a solution of NaOH (10 g, 250 mmol) in water (30 mL) was added to the reaction mixture. After it was stirred for an additional 30 min at room temperature, the mixture was extracted with several portions of diethyl ether. The organic layers were combined and dried over anhydrous MgSO₄, and solvent was removed in vacuo. The resulting yellow oil was heated in vacuo (90 °C, 300 mTorr) in order to remove any excess H₂N(2,6-i-Pr₂C₆H₃). The remaining viscous orange oil was essentially pure product (7.26 g, 82%); no further purification was necessary: ¹H NMR δ 7.10 (m, 6, H_{aryl}), 3.42 (sept, 4, CHMe₂), 2.98 (t, 4, NCH₂), 2.64 (t, 4, CH₂S), 1.23 (d, 24, CHMe₂).

[2a]Zr(NMe₂)₂. A solution of Zr(NMe₂)₄ (0.81 g, 3.04 mmol) in pentane (4 mL) and a solution of H₂[2a] (1.0 g, 3.04 mmol) in pentane (14 mL) and toluene (2 mL) were combined and allowed to stand for 20 h at room temperature. The solvent was removed in vacuo, and the remaining oily yellow residue was washed several times with pentane to remove all remaining traces of toluene. Recrystallization from pentane at -35 °C gave 1.21 g (79%) of off-white crystals: ¹H NMR δ 7.10 (d, 4, H_m), 6.90 (t, 2, H_p), 3.31 (br s), 2.54 (t), 2.40 (s); ¹H NMR (toluene-*d*₈, 100 °C) δ 6.98 (d, 4, H_m), 6.79 (t, 2, H_p), 3.39 (t, 4, NCH₂), 2.73 (t, 4, CH₂S), 2.58 (br s, 12, ZrNMe₂), 2.37 (s, 12, ArMe); ¹³C{¹H} NMR δ 152.9 (C_{ipso}), 135.1 (C_o), 129.0 (C_m), 123.9 (C_p), 56.7 (NCH₂), 43.3 (br, ZrNMe₂), 36.2 (CH₂S), 19.7 (ArMe). Anal. Calcd for C₂₄H₃₈N₄SZr: C, 56.98; H, 7.57; N, 11.08. Found: C, 57.02; H, 7.50; N, 10.85.

[2a]ZrCl₂. Neat Me₃SiCl (6.1 mL, 48 mmol) was added to a solution of **[2a]Zr(NMe₂)₂** (1.21 g, 2.39 mmol) in 80 mL of diethyl ether at room temperature, and the mixture was shaken vigorously. After approximately 48 h pale yellow crystals were isolated in 97% yield: ¹H NMR (CD₂Cl₂) 7.08 (m, 6, H_{aromat}), 4.23 (m, 2), 3.60–3.38 (m, 6), 2.40 (s, 6, ArMe), 2.42 (s, 6, ArMe); ¹³C{¹H} NMR (CD₂Cl₂) δ 146.2 (C_{ipso}), 136.1 (C_o), 135.7 (C_o), 129.6 (C_m), 129.4 (C_m), 127.2 (C_p), 59.2 (NCH₂), 34.3 (CH₂S), 19.32 (ArMe), 19.28 (ArMe). Anal. Calcd for C₂₀H₂₆Cl₂N₂SZr: C, 49.16; H, 5.36; N, 5.73. Found: C, 48.89; H, 5.40; N, 5.63.

[2a]ZrMe₂. A chilled (-30 °C) solution of MeMgBr (3.0 M in ether, 0.35 mL, 1.05 mmol) was added to a suspension of **[2a]ZrCl₂** (0.250 g, 0.512 mmol) in diethyl ether (6 mL) at -30 °C. The reaction mixture was warmed to room temperature and was stirred for 20 min. 1,4-Dioxane (92 μL, 1.08 mmol) was added, and the mixture was stirred at room temperature for an additional 10 min. The mixture was then filtered through Celite, and the solvent was removed from the filtrate in vacuo. The white residue was recrystallized from pentane at -35 °C to give the product in 71% yield: ¹H NMR δ 7.01 (d, 4, H_m), 6.98 (t, 2, H_p), 3.35 (br s), 2.44 (m), 0.29 (br s); ¹H NMR (toluene-*d*₈, 50 °C) δ 7.02 (d, 4, H_m), 6.93 (t, 2, H_p), 3.38 (t, 4, NCH₂), 2.57 (t, 4, CH₂S), 2.40 (s, 12, ArMe), 0.02 (br s, 6, ZrMe₂); ¹³C{¹H} NMR δ 146.3 (C_{ipso}), 137.0 (C_o), 129.5 (C_m), 126.4 (C_p), 57.6 (NCH₂), 33.5 (CH₂S), 19.5 (ArMe).

¹³CH₃MgI (1.1M in diethyl ether) was used to prepare **[2a]-Zr**(¹³CH₃)₂: ¹³C NMR (CD₂Cl₂, -40 °C) δ 41.0, 37.5.

[2c]Zr(NMe₂)₂. A solution of Zr(NMe₂)₄ (3.22 g, 7.31 mmol) in toluene (15 mL) was added to a solution of H₂[2c] (1.95 g, 7.31 mmol) in toluene (35 mL) at room temperature, and the mixture was heated to 110 °C overnight. After approximately 20 h at 110 °C the solvent was removed in vacuo. The remaining orange oil was washed with several portions of pentane to ensure removal of all traces of toluene. The oily yellow solid was recrystallized from pentane at -35 °C to

afford large yellow crystals in 66% yield: ^1H NMR δ 7.15 (m, H_{aryl}), 3.71 (br m), 3.50 (br s), 2.54 (br m), 1.36 (d, 12, CHMe_2), 1.24 (d, 12, CHMe_2); ^1H NMR (toluene- d_6 , 100 $^\circ\text{C}$) δ 7.17–6.92 (m, 6, H_{aryl}), 3.69 (sept, 4, CHMe_2), 3.56 (t, 4, NCH_2), 2.71 (t, 4, CH_2S), 2.56 (br s, 12, ZrNMe_2), 1.31 (d, 12, CHMe_2), 1.22 (d, 12, CHMe_2); $^{13}\text{C}\{^1\text{H}\}$ NMR δ 150.3 (C_{ipso}), 146.4 (C_o), 125.5 (C_m), 124.4 (C_p), 59.8 (NCH_2), 44.5 (br, ZrNMe_2), 36.0 (CH_2S), 28.8 (CHMe_2), 27.1 (CHMe_2), 24.9 (CHMe_2).

[2c]ZrCl₂. Neat TMSCl (2.37 mL, 18.71 mmol) was added to a room-temperature solution of **[2c]Zr(NMe₂)₂** (0.410 g, 0.66 mmol) in diethyl ether (10 mL). The resulting yellow solution was stirred at room temperature for approximately 48 h. A white precipitate was observed after several hours. After the mixture was stirred at room temperature over two nights, solvent was removed in vacuo, affording 0.317 g (79%) of white powder: ^1H NMR (CDCl_3 , room temperature) δ 7.26 (m, 6, H_{aromat}), 4.35 (m, 2), 3.70 to 3.40 (m, 10), 1.38 (d, 6, CHMe_2), 1.35 (d, 6, CHMe_2), 1.25 (d, 6, CHMe_2), 1.20 (d, 6, CHMe_2); $^{13}\text{C}\{^1\text{H}\}$ NMR (CDCl_3) δ 145.5 (C_{ipso}), 144.6 (C_o), 127.4 (C_m), 124.6 (C_p), 61.5 (NCH_2), 34.0 (CH_2S), 29.0 (CHMe_2), 28.3 (CHMe_2), 27.2 (CHMe_2), 27.0 (CHMe_2), 24.6 (CHMe_2), 23.8 (CHMe_2). Anal. Calcd for $\text{C}_{28}\text{H}_{42}\text{N}_2\text{SZrCl}_2$: Cl, 11.80. Found: Cl, 12.07.

[2c]ZrMe₂. A chilled solution of MeMgBr (3.0 M in ether, 0.352 mL, 1.06 mmol) was added to a suspension of **[2c]ZrCl₂** (0.317 g, 0.527 mmol) in diethyl ether (15 mL) at -35 $^\circ\text{C}$. The reaction mixture was stirred at room temperature for 45 min. 1,4-Dioxane (0.09 mL, 1.06 mmol) was added, and after 15 min the mixture was filtered through Celite. The solvent was removed from the filtrate in vacuo, and the residue was recrystallized from diethyl ether at -30 $^\circ\text{C}$ to yield white crystals in 73% yield: ^1H NMR δ 7.18 (m, H_{aryl}), 3.8 (br s), 3.55 (br s), 2.51 (t), 1.40 (d, 12, CHMe_2), 1.20 (d, 12, CHMe_2), 0.35 (br s); ^1H NMR (toluene- d_6 , 60 $^\circ\text{C}$) δ 7.15–6.94 (m, 6, H_{aryl}), 3.80 (br, 4, CHMe_2), 3.60 (br, 4, NCH_2), 2.65 (br, 4, CH_2S), 1.38 (d, 12, CHMe_2), 1.21 (d, 12, CHMe_2), 0.16 (br s, 6, ZrMe_2); $^{13}\text{C}\{^1\text{H}\}$ NMR δ 147.1 (C_{ipso}), 145.3 (C_o), 127.1 (C_m), 124.9 (C_p), 60.7 (NCH_2), 33.9 (CH_2S), 29.1 (CHMe_2), 27.4 (CHMe_2), 24.8 (CHMe_2). Anal. Calcd for $\text{C}_{30}\text{H}_{48}\text{N}_2\text{SZr}$: C, 64.34; H, 8.64; N, 5.00. Found: C, 64.46; H, 8.57; N, 4.91.

$^{13}\text{CH}_3\text{MgI}$ (1.1 M in diethyl ether) was used to prepare **[2c]-Zr($^{13}\text{CH}_2$)₂**: $^{13}\text{C}\{^1\text{H}\}$ NMR (C_6D_6 , 0 $^\circ\text{C}$) δ 45.59, 39.39.

[2c]Zr(i-Bu)₂. A chilled solution of $\text{ClMgCH}_2\text{CHMe}_2$ (2.0 M in ether, 0.62 mL, 1.24 mmol) was added to a solution of **[2c]ZrCl₂** (0.373 g, 0.62 mmol) in diethyl ether (15 mL) at -35 $^\circ\text{C}$. The reaction was carried out as outlined for **[2c]ZrMe₂** to give pale yellow crystals of the product in 46% yield: ^1H NMR δ 7.18 (m, H_{aromat}), 3.82 (br s), 3.77 (br s), 2.50 (br s), 1.46 (d), 1.20 (d), 0.81 (br s); ^1H NMR (toluene- d_6 , 80 $^\circ\text{C}$) δ 7.19 to 6.91 (m, 6, H_{aromat}), 3.84 (br, 4, PhCHMe_2), 3.63 (br, 4, NCH_2), 2.66 (br, 4, CH_2S), 1.84 (br, 2, CH_2CHMe_2), 1.44 (d, 12, PhCHMe_2), 1.21 (d, 12, PhCHMe_2), 0.83 (m, 12, CH_2CHMe_2), 0.59 (br, 4, ZrCH_2); $^{13}\text{C}\{^1\text{H}\}$ NMR δ 147.9 (C_{ipso}), 146.6 (C_o), 127.3 (C_p), 125.1 (C_m), 81.7 (br, CH_2CHMe_2), 61.4 (CH_2N), 34.7 (SCH_2), 31.9 (br, CH_2CHMe_2), 29.0 (CHMe_2), 28.4 (CH_2CHMe_2), 27.8 (CHMe_2), 24.6 (CHMe_2).

Generation of {[1a]ZrMe(PhNMe₂)}[B(C₆F₅)₄]. Solid **[1a]ZrMe₂** (13 mg, 0.030 mmol) was added to a chilled (-30 $^\circ\text{C}$) suspension of $[\text{PhNMe}_2\text{H}][\text{B}(\text{C}_6\text{F}_5)_4]$ (24 mg, 0.030 mmol) in $\text{C}_6\text{D}_5\text{Cl}$. The reaction mixture was stirred for 5 min while it was warmed to room temperature and then chilled to 0 $^\circ\text{C}$: ^1H NMR ($\text{C}_6\text{D}_5\text{Cl}$) δ 0.26 (s, 3, ZrMe), 2.22 (s, 12, ArMe), 2.67 (s, 6, PhNMe_2), 3.10 (m, 2, CH_2N), 3.41 (m, 2, CH_2N), 3.95 (m, 2, OCH_2), 4.12 (m, 2, OCH_2), [5.79 (d, 2), 6.03 (br, 3H)] (PhNMe_2), 7.13 (m, 6, H_{aryl}).

Generation of {[1c]ZrMe(PhNMe₂)}[B(C₆F₅)₄]. Solid **[1c]ZrMe₂** (20 mg, 0.037 mmol) was added to a chilled (-30 $^\circ\text{C}$) suspension of $[\text{PhNMe}_2\text{H}][\text{B}(\text{C}_6\text{F}_5)_4]$ (29 mg, 0.037 mmol) in $\text{C}_6\text{D}_5\text{Cl}$. The reaction mixture was stirred for 5 min while it was warmed to room temperature and then chilled to 0 $^\circ\text{C}$: ^1H NMR ($\text{C}_6\text{D}_5\text{Cl}$) δ 0.22 (s, 3, ZrMe), 1.16 (d, 6, CHMe_2), 1.24 (d, 6, CHMe_2), 1.35 (d, 6, CHMe_2), 1.45 (d, 6, CHMe_2), 2.80 (s,

6, PhNMe_2), 3.23 (heptet, 4, CHMe_2), 3.33 (m, 2, CH_2N), 3.73 (m, 2, CH_2N), 3.98 (m, 2, OCH_2), 4.22 (m, 2, OCH_2), [5.85 (m, 4), 6.33 (br t, 1H)] (PhNMe_2), 7.11–7.27 (m, 6, H_{aryl}).

Generation of {[1c]HfMe(PhNMe₂)}[B(C₆F₅)₄]. **[1c]-HfMe₂** (16 mg, 0.025 mmol) and $[\text{PhNMe}_2\text{H}][\text{B}(\text{C}_6\text{F}_5)_4]$ (20 mg, 0.025 mmol) were combined in 0.8 mL of $\text{C}_6\text{D}_5\text{Br}$ at -30 $^\circ\text{C}$. The reaction mixture was stirred for 10 min while being warmed to room temperature, after which it was chilled to -20 $^\circ\text{C}$: ^1H NMR ($\text{C}_6\text{D}_5\text{Br}$, -20 $^\circ\text{C}$) δ -0.17 (s, 3, HfMe), 1.07 (d, 6, CHMe_2), 1.11 (d, 6, CHMe_2), 1.20 (d, 6, CHMe_2), 1.33 (d, 6, CHMe_2), 2.62 (s, 6, PhNMe_2), 3.01 (heptet, 2, CHMe_2), 3.15 (heptet, 2, CHMe_2), 3.20 (dt, 2, CH_2N), 3.55 (br, 2, CH_2N), 3.78 (br, 2, OCH_2), 4.01 (br, 2, OCH_2), [5.62 (m, 2), 5.74 (t, 2), 6.06 (t, 1H)] (PhNMe_2), 7.05–7.22 (m, 6, H_{aryl}).

Generation of {[1a]ZrMe(ether)}[B(C₆F₅)₄]. To a chilled (-30 $^\circ\text{C}$) suspension of $[\text{PhNMe}_2\text{H}][\text{B}(\text{C}_6\text{F}_5)_4]$ (80 mg, 0.1 mmol) in 2.5 mL of $\text{C}_6\text{H}_5\text{Cl}$ was added a similarly precooled solution of **[1a]ZrMe₂** (43 mg, 0.1 mmol) in 2.5 mL of $\text{C}_6\text{H}_5\text{Cl}$. The reaction mixture was periodically mixed by shaking and was warmed slowly to room temperature. After 30 min all the $[\text{PhNMe}_2\text{H}][\text{B}(\text{C}_6\text{F}_5)_4]$ dissolved. Ether (1 mL) and then 15 mL of pentane were then added, which led to bleaching of the color, formation of an opaque solution, and slow precipitation of an oily product. When the reaction mixture was cooled to -30 $^\circ\text{C}$, the oil was transformed into tiny dendritic pale beige microcrystals. These were separated, washed with two 5 mL portions of pentane/ether (1:1), and dried in vacuo to yield 98 mg (84%) of light white powder. The compound is thermally unstable both in solution and in the solid state and should be stored at -30 $^\circ\text{C}$: ^1H NMR ($\text{C}_6\text{D}_5\text{Br}$) δ 0.21 (t, 6, $\text{O}(\text{CH}_2\text{Me})_2$), 0.40 (s, 3, ZrMe), 1.93 (s, 6, ArMe), 2.22 (s, 6, ArMe), 2.80 (q, 4, $\text{O}(\text{CH}_2\text{Me})_2$), 3.15 (dt, 2, CH_2N), 3.48 (m, 2, CH_2N), 3.87 (m, 2, OCH_2), 4.05 (m, 2, OCH_2), 6.88–7.00 (m, 6, H_{aryl}); $^{13}\text{C}\{^1\text{H}\}$ NMR ($\text{C}_6\text{D}_5\text{Br}$) δ 11.74 ($\text{O}(\text{CH}_2\text{Me})_2$), 17.98 (ArMe), 18.10 (ArMe), 40.57 (ZrMe), 54.81 (CH_2N), 68.22 ($\text{O}(\text{CH}_2\text{Me})_2$), 74.32 (OCH_2), [127.78, 129.99, 134.28, 136.28, 140.90] (C_{aryl}), [136.4 (dm), 138.3 (dm), 148.5 (dm)] (C_6F_5) (one resonance belonging to an aryl carbon and one belonging to a C_6F_5 carbon were not found, probably because of the overlap with the resonances of the solvent); $^{19}\text{F}\{^1\text{H}\}$ NMR ($\text{C}_6\text{D}_5\text{Br}$) δ -166.31 (m, F_m), -162.44 (t, F_p), -132.17 (br, F_o).

Generation of {[1a]HfMe(ether)}[B(C₆F₅)₄]. The procedure, molar amounts of the reactants, and observations were similar to those described for the preparation of $\{[\mathbf{1a}]\text{ZrMe}(\text{ether})\}[\text{B}(\text{C}_6\text{F}_5)_4]$, but due to much higher thermal stability of the Hf complexes involved, no cooling was necessary. $\{[\mathbf{1a}]\text{-HfMe}(\text{Et}_2\text{O})\}[\text{B}(\text{C}_6\text{F}_5)_4]$ was formed in 82% yield as colorless microcrystals: ^1H NMR ($\text{C}_6\text{D}_5\text{Br}$) δ 0.17 (t, 6, $\text{O}(\text{CH}_2\text{Me})_2$), 0.36 (s, 3, HfMe), 2.01 (s, 6, ArMe), 2.22 (s, 6, ArMe), 2.80 (q, 4, $\text{O}(\text{CH}_2\text{Me})_2$), 3.20 (dt, 2, CH_2N), 3.46 (m, 2, CH_2N), 3.86 (m, 2, OCH_2), 4.02 (m, 2, OCH_2), 6.88–6.98 (m, 6, H_{aryl}); $^{13}\text{C}\{^1\text{H}\}$ NMR ($\text{C}_6\text{D}_5\text{Br}$) δ 11.32 ($\text{O}(\text{CH}_2\text{Me})_2$), 17.89 (ArMe), 18.28 (ArMe), 45.49 (HfMe), 54.31 (CH_2N), 68.59 ($\text{O}(\text{CH}_2\text{Me})_2$), 75.04 (OCH_2), [127.07, 134.10, 135.49, 142.57] (C_{aryl}), [136.4 (dm), 138.4 (dm), 148.5 (dm)] (C_6F_5); two resonances belonging to an aryl carbon and one belonging to a C_6F_5 carbon were not found, probably because of the overlap with the resonances of the solvent); $^{19}\text{F}\{^1\text{H}\}$ NMR ($\text{C}_6\text{D}_5\text{Br}$) δ -165.95 (t, 2F_{meta}), -162.06 (t, 1F_{para}), -131.83 (br, 2F_{ortho}).

Generation of {[2a]ZrMe(THF)}[B(C₆F₅)₄]. Solid **[2a]-ZrMe₂** (17 mg, 37 μmol) was added to a solution of $[\text{PhNMe}_2\text{H}][\text{B}(\text{C}_6\text{F}_5)_4]$ (29 mg, 37 μmol) in $\text{C}_6\text{D}_5\text{Br}$ (0.7 mL) at -35 $^\circ\text{C}$. The yellow solution was stirred at room temperature for 5 min, during which time the color changed to brown. A drop of THF was added, and the solution changed color to bright yellow: ^1H NMR ($\text{C}_6\text{D}_5\text{Br}$) δ 7.2 (t, 2, free PhNMe_2), 6.94 (m, H_{aryl}), 6.72 (t, 1, free PhNMe_2), 6.60 (d, 2, free PhNMe_2), 3.63 (m, 2, $\text{NCH}_2\text{CH}_2\text{S}$), 3.42 (m, THF), 3.35 (m, 2, $\text{NCH}_2\text{CH}_2\text{S}$), 2.96 (m, 4, $\text{NCH}_2\text{CH}_2\text{S}$), 2.61 (s, 6, free PhNMe_2), 2.20 (s, 6, PhCH_3), 1.89 (s, 6, PhCH_3), 1.48 (m, THF), 0.20 (s, 3, ZrMe).

Polymerization of 1-Hexene using [2a,c]ZrR₂ Com-

plexes. In a typical experiment, 10 mmol of 1-hexene (1.25 mL) was added to a solution of 50 μ mol of **[2a]**ZrMe₂ (0.022 g) and 50 μ mol of [PhNMe₂H][B(C₆F₅)₄] (0.039 g) in chlorobenzene (13 mL) was added at 0 °C. After 3 h the reaction was quenched by addition of HCl in diethyl ether (4 mL, 1.0 M). Most solvent was removed at 15 Torr (water aspirator) at 50 °C, and the viscous oil was dried at approximately 200 mTorr at 60 °C for 18–20 h.

Polymerization Experiments. (a) Preparative Scale Polymerizations of 1-Hexene using Zr and Hf Catalysts.

To a chilled (–30 °C) solution of **[1a–d]**MMe₂ (M = Zr, Hf) (0.040 mmol) in chlorobenzene (4 mL) was added a solution of [Ph₃C][B(C₆F₅)₄] (40 mmol) in chlorobenzene (6 mL) at –30 °C, and the reaction mixture was stirred for 5 min. The reaction mixture was allowed to equilibrate at 0 °C, and an appropriate amount of 1-hexene was added in one shot. After the mixture was stirred for 1 h at 0 °C, the reaction was quenched with HCl (1.0 M in ether, 4 mL). All volatile components were removed in vacuo (100 mTorr) at 120 °C. Experiments with [PhNMe₂H][B(C₆F₅)₄] as an initiator were carried out similarly, but prior to the addition of the monomer the reaction mixture was stirred for 15 min while being warmed to room temperature to ensure complete dissolution of the initiator and its reaction with the metal complex. The GPC and polymer yield data are compiled in Table 3.

(b) Attempted Polymerization of Ethylene using {[1a]-MMe(Et₂O)}[B(C₆F₅)₄] (M = Zr, Hf). A solution of 0.01 mmol of a metal complex in 10 mL of chlorobenzene was stirred at 0 °C under 1 atm of ethylene for 10 min in a weighed flask. The reaction was quenched with HCl (1.0 M in ether, 4 mL). After all volatile components were removed in vacuo,

the reaction flask was weighed again to show a negligible increase in mass (less than 10 mg).

(c) NMR Scale Polymerization of 1-Hexene using Ti Catalysts. To a solution of **[1a]**TiMe₂ (19 mg, 0.049 mmol) in 0.6 mL of C₆D₅Br was added at –30 °C a suspension of [PhNMe₂H][B(C₆F₅)₄] (40 mg, 0.05 mmol) in 0.15 mL of C₆D₅-Br. The mixture was stirred at room temperature for 15 min, over which time the color changed from yellow to dark red. The solution was precooled again to –30 °C, and to it was added 155 μ L (105 mg, 25 equiv) of 1-hexene. The reaction mixture was transferred to an NMR tube and was kept in an ice bath at 0 °C. Periodic monitoring by ¹H NMR allowed us to follow the course of the polymerization reaction. After 3.5 h the yield of the polymer was roughly estimated by ¹³C{¹H} NMR to be ~75%. After overnight the monomer was still not fully consumed. The experiment utilizing **[1a]**Ti(CH₂Ph)₂ was carried out completely analogously and yielded similar results.

Acknowledgment. R.R.S. thanks the Department of Energy (DE-FG02-86ER13564) and Exxon for supporting this research, and M.A. is grateful for a one-year Rueff-Wormser Postdoctoral Fellowship.

Supporting Information Available: Figures giving additional views and tables giving crystal data and structure refinement details, atomic coordinates, bond distances and angles, and thermal parameters for **[1a]**Ti(CH₂Ph)₂, **[1a]**ZrMe₂, **[1c]**HfEt₂, and **[2a]**ZrMe₂ (23 pages). Ordering information is given on any current masthead page.

OM980512A